RESEARCH ARTICLE

Transcription factor binding site clusters identify target genes with similar tissue-wide expression and buffer against mutations [version 1; peer review: 2 approved with reservations]

Ruipeng Lu[1], Peter K. Rogan[1-3]

[1]Computer Science, University of Western Ontario, London, Ontario, N6A 5B7, Canada
[2]Biochemistry, University of Western Ontario, London, Ontario, N6A 5C1, Canada
[3]Cytognomix, London, Ontario, N5X 3X5, Canada

v1 **First published:** 14 Dec 2018, **7**:1933 (https://doi.org/10.12688/f1000research.17363.1)
Latest published: 08 Apr 2019, **7**:1933 (https://doi.org/10.12688/f1000research.17363.2)

Abstract

Background: The distribution and composition of *cis*-regulatory modules composed of transcription factor (TF) binding site (TFBS) clusters in promoters substantially determine gene expression patterns and TF targets. TF knockdown experiments have revealed that TF binding profiles and gene expression levels are correlated. We use TFBS features within accessible promoter intervals to predict genes with similar tissue-wide expression patterns and TF targets.

Methods: Genes with correlated expression patterns across 53 tissues and TF targets were respectively identified from Bray-Curtis Similarity and TF knockdown experiments. Corresponding promoter sequences were reduced to DNase I-accessible intervals; TFBSs were then identified within these intervals using information theory-based position weight matrices for each TF (iPWMs) and clustered. Features from information-dense TFBS clusters predicted these genes with machine learning classifiers, which were evaluated for accuracy, specificity and sensitivity. Mutations in TFBSs were analyzed to *in silico* examine their impact on cluster densities and the regulatory states of target genes.

Results: We initially chose the glucocorticoid receptor gene (*NR3C1*), whose regulation has been extensively studied, to test this approach. *SLC25A32* and *TANK* were found to exhibit the most similar expression patterns to *NR3C1*. A Decision Tree classifier exhibited the largest area under the Receiver Operating Characteristic (ROC) curve in detecting such genes. Target gene prediction was confirmed using siRNA knockdown of TFs, which was found to be more accurate than those predicted after CRISPR/CAS9 inactivation. *In-silico* mutation analyses of TFBSs also revealed that one or more information-dense TFBS clusters in promoters are required for accurate target gene prediction.

Conclusions: Machine learning based on TFBS information density, organization, and chromatin accessibility accurately identifies gene targets with comparable tissue-wide expression patterns. Multiple information-dense TFBS clusters in promoters appear to protect promoters from effects of deleterious binding site mutations in a single TFBS that would otherwise alter regulation of these genes.

Open Peer Review

Referee Status: ? ✓

	Invited Referees 1	2
REVISED version 2 published 08 Apr 2019		✓ report
version 1 published 14 Dec 2018	? report	? report

1 **Daphne Ezer**, The Alan Turing Institute for Data Science, UK

2 **Nicolae Radu Zabet**, University of Essex, UK

Any reports and responses or comments on the article can be found at the end of the article.

Keywords
Transcription factors, position-specific scoring matrices, chromatin, binding sites, gene expression profiles, Bray-Curtis similarity, mutation, machine learning, information theory

Corresponding author: Peter K. Rogan (progan@uwo.ca)

Author roles: Lu R: Conceptualization, Data Curation, Formal Analysis, Methodology, Resources, Software, Validation, Visualization, Writing – Original Draft Preparation, Writing – Review & Editing; **Rogan PK**: Conceptualization, Formal Analysis, Funding Acquisition, Methodology, Project Administration, Supervision, Writing – Original Draft Preparation, Writing – Review & Editing

Competing interests: PKR is the inventor of US Patent 5,867,402 and other patents pending, which apply iPWMs to the prediction and validation of mutations. He cofounded Cytognomix, Inc., which is developing software based on this technology for complete genome or exome mutation analysis.

Grant information: Natural Sciences and Engineering Research Council of Canada Discovery Grant [RGPIN-2015-06290]; Canada Foundation for Innovation; Canada Research Chairs; Cytognomix Inc. Compute Canada and Shared Hierarchical Academic Research Computing Network (SHARCNET) provided high performance computing and storage facilities. Funding for open access charge: University of Western Ontario and the Natural Sciences and Engineering Research Council.
The funders had no role in study design, data collection and analysis, decision to publish, or preparation of the manuscript.

How to cite this article: Lu R and Rogan PK. **Transcription factor binding site clusters identify target genes with similar tissue-wide expression and buffer against mutations [version 1; peer review: 2 approved with reservations]** F1000Research 2018, **7**:1933 (https://doi.org/10.12688/f1000research.17363.1)

First published: 14 Dec 2018, **7**:1933 (https://doi.org/10.12688/f1000research.17363.1)

Introduction

The distinctive organization and combination of transcription factor binding sites (TFBSs) and regulatory modules in promoters dictates specific expression patterns within a set of genes[1]. Clustering of multiple adjacent binding sites for the same TF (homotypic clusters) and for different TFs (heterotypic clusters) defines *cis*-regulatory modules (CRMs) in human gene promoters. Experimental studies have shown that these clusters can reinforce (and in some instances, amplify) the impact of individual TFBSs on gene expression through increasing binding affinities, facilitated diffusion mechanisms and funnel effects[2]. Because tissue-specific TF-TF interactions in TFBS clusters are prevalent, these features can assist in identifying correct target genes by altering binding specificities of individual TFs[3]. Previously, we derived iPWMs from ChIP-seq data that can accurately detect TFBSs and quantify their strengths by computing associated R_i values (Rate of Shannon information transmission for an individual sequence[4]), with $R_{sequence}$ being the average of R_i values of all binding site sequences and representing the average binding strength of the TF[3]. Furthermore, information density-based clustering (IDBC) can effectively identify functional TF clusters by taking into account both the spatial organization (i.e. intersite distances) and information density (i.e. R_i values) of TFBSs[5].

TF binding profiles, either derived from *in vivo* ChIP-seq peaks[6–8] or computationally detected binding sites and CRMs[9], have been shown to be predictive of absolute gene expression levels using a variety of tissue-specific machine learning classifiers and regression models. Because signal strengths of ChIP-seq peaks are not strictly proportional to TFBS strengths[3], representing TF binding strengths by ChIP-seq signals may not be appropriate; nevertheless, both achieved similar accuracy[10]. CRMs have been formed by combining two or three adjacent TFBSs[9], which is inflexible, as it arbitrarily limits the number of binding sites contained in a module, and does not consider differences between information densities of different CRMs. Chromatin structure (e.g. histone modification (HM) and DNase I hypersensitive sites (DHSs)) were also found to be statistically redundant with TF binding in explaining tissue-specific mRNA transcript abundance at a genome-wide level[7,8,11,12], which was attributed to the heterogeneous distribution of HMs across chromatin domains[8]. Combining these two types of data explained the largest fraction of variance in gene expression levels in multiple cell lines[7,8], suggesting that either contributes unique information to gene expression that cannot be compensated for by the other.

The number of genes directly bound by a TF significantly exceeds the number of differentially expressed (DE) genes whose expression levels significantly change upon knockdown of the TF. Only a small subset of direct target genes whose promoters overlap ChIP-seq peaks were DE after individually knocking 59 TFs down using small interfering RNAs (siRNAs) in the GM19238 cell line[13]. Using these knockdown data on 8,872 genes as the gold standard, correlation between TFBS counts and gene expression levels across 10 different cell lines was more predictive of DE targets than setting a minimum threshold on TFBS counts[14]. Their TFBS counts were defined as the number of ChIP-seq peaks overlapping the promoter, though it was unknown how many binding sites were present in these peaks; positives might not be direct targets in the TF regulatory cascade, as the promoters of these targets were not intersected with ChIP-seq peaks. By perturbing gene expression with CAS9-directed clustered regularly interspaced short palindromic repeats (CRISPR) of 10 different TF genes in K562 cells, the regulatory effects of each TF on 22,046 genes were dissected by single cell RNA sequencing with a regularized linear computational model[15]; this accurately revealed DE targets and new functions of individual TFs, some of which were likely regulated through direct interactions at TFBSs in their corresponding promoters. Machine learning classifiers have also been applied in a small number of gene instances to predict targets of a single TF using features extracted from *n*-grams derived from consensus binding sequences[16], or from TFBSs and homotypic binding site clusters[5].

To investigate whether the distribution and composition of CRMs in promoters substantially determines gene expression profiles of direct TF targets, we developed a general machine learning framework that predicts which genes have similar tissue-wide expression profiles to a given gene and predicts DE direct TF targets by combining information theory-based TF binding profiles with DHSs. Upon filtering of accessible promoter intervals based on the locations of DHSs, features designed to capture the spatial distribution and information composition of CRMs were extracted from clusters of iPWM-detected TFBSs identified by IDBC. Though not all direct targets regulated by multiple TFs share a common tissue-wide expression profile, this framework provides insight into the transcriptional program of genes with similar profiles by dissecting their *cis*-regulatory element organization and strengths. We identify genes with comparable tissue-wide expression profiles by application of Bray-Curtis similarity[17]. Using transcriptome data generated by CRISPR-[15] and siRNA-based[13] TF knockdowns, we predicted DE TF target genes that are simultaneously direct targets whose promoters overlap tissue-specific ChIP-seq peaks.

Methods

To identify genes with similar tissue-wide expression patterns, we formally define tissue-wide gene expression profiles and pairwise similarity measures between profiles of different genes. A general machine learning framework relates features extracted from the organization of TFBSs in these genes to their tissue-wide expression patterns. Since protein-coding (PC) sequences represent the most widely studied and best understood component of the human genome[18], positives and negatives for deriving machine learning classifiers for predicting DE direct TF target genes that encode proteins (TF targets for short below) were obtained from CRISPR- and siRNA-generated knockdown data (see below).

Similarity between GTEx tissue-wide expression profiles of genes

The Genotype-Tissue Expression (GTEx, version 6p) Project measured expression levels in 53 tissues, each of which is represented by different numbers of individuals (5 to 564). For

each tissue population, the median expression value is given in RPKM (Reads Per Kilobase of transcript per Million mapped reads) for each gene[19]. Data are available on Zenodo[20]. To capture the tissue-wide overall expression pattern of a gene instead of within a single tissue, the tissue-wide expression profile of a gene was defined as its median RPKM across GTEx tissues, which is described by a 53 element vector (Equation 1). Note that different isoforms whose expression patterns may significantly differ from each other cannot be distinguished by this approach.

$$EP^A = [MEV_1^A, MEV_2^A, \cdots, MEV_{53}^A] \ (in\ RPKM) \quad (1)$$

where EP^A is the tissue-wide expression profile of Gene A, MEV_1^A is the median expression value of Gene A in Tissue 1, MEV_2^A is the median expression value of Gene A in Tissue 2, etc.

To discover other genes whose tissue-wide expression profiles are similar to a given gene, we computed the Bray-Curtis Similarity (Equation 2) between the tissue-wide expression profiles of gene pairs. Compared to other similarity metrics (Table 1, Example 1, Additional file 1[21]), the application of this function is justified by desirable properties, including: 1) maintaining bounds between 0 and 1, 2) achieving the maximal similarity value 1 if and only if two vectors are identical, and 3) larger values having a larger impact on the resultant similarity value.

$$sim_{Bray-Curtis}(EP^A, EP^B) = \begin{cases} 1, & if \ \sum_{i=1}^{53} MEV_i^A = \sum_{i=1}^{53} MEV_i^B = 0 \\ 1 - \frac{\sum_{i=1}^{53} |MEV_i^A - MEV_i^B|}{\sum_{i=1}^{53} (MEV_i^A + MEV_i^B)}, & otherwise \end{cases} \quad (2)$$

Example 1. Assume that Genes A,B,C,D,E,F respectively have the following GTEx expression profiles across two tissues: EP^A = [1,1], EP^B =[2,2], EP^C = [3,3], EP^D = [1,2], EP^E = [1,99], EP^F = [1,100]. The ground-truth similarity relationships that we can intuitively infer include $sim(EP^C, EP^A) < sim(EP^C, EP^B) < 1$, and $sim(EP^A, EP^D) < sim(EP^E, EP^F) < 1$. Only the results computed by the Bray-Curtis Similarity are completely concordant with these ground-truth relationships (Table 2).

Prediction of genes with similar tissue-wide expression profiles

The framework for identifying genes whose tissue-wide expression profiles most resemble a particular gene is shown in Figure 1A, B. The genomic locations of all DHSs in 95 cell types generated by the ENCODE project[22; hg38 assembly] were selected for known promoters[23], then 94 iPWMs exhibiting primary binding motifs for 82 TFs[3] were used to detect TFBSs within the overlapping intervals. Data are available on Zenodo[20]. When detecting heterotypic TFBS clusters with the IDBC algorithm, a minimum threshold 0.1 * $R_{sequence}$ was specified for the R_i values of TFBSs in order to remove weak binding sites that were more likely to be false positive TFBSs[3].

Table 1. Comparison between metrics in measurement of similarity between GTEx tissue-wide expression profiles of genes.

Similarity metric	Property 1†,‡	Property 2†	Property 3†
Bray-Curtis	√; [0,1]	√	√
Euclidean	√; (0,1]	√	×
Cosine	√; [0,1]	×	√
Pearson correlation[24]	×; [-1,1]	×	×
Spearman correlation[25]	×; [-1,1]	×	×

† The symbols √ and ×, respectively, indicate that the similarity metric satisfies and does not satisfy the property. ‡The interval in each cell indicates the range in which the result computed by the similarity metric lies.

Table 2. Similarity values computed by different metrics.

Similarity metric	$sim(EP^C, EP^B)$	$sim(EP^C, EP^A)$	$sim(EP^E, EP^F)$	$sim(EP^A, EP^D)$
Bray-Curtis	0.8	0.5	≈ 0.995	0.8
Euclidean	≈ 0.41	≈ 0.26	0.5	0.5
Cosine	1	1	≈ 0.999999995	≈ 0.949
Pearson correlation	Undefined	Undefined	1	1
Spearman correlation	1	1	1	1

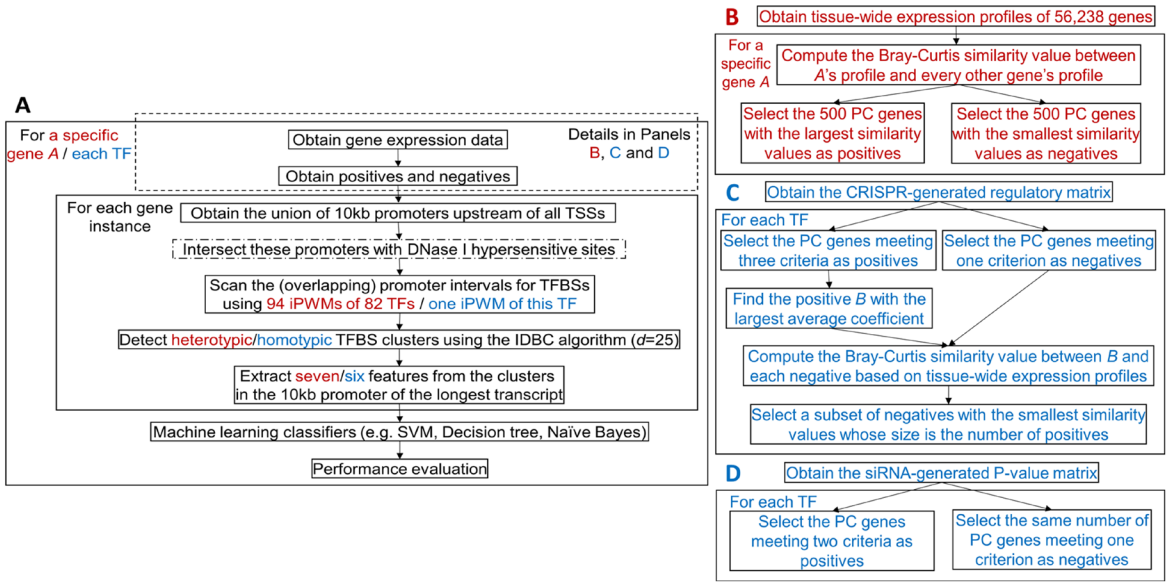

Figure 1. The general framework for predicting genes with similar tissue-wide expression profiles and TF targets. Red and blue contents are respectively specific to prediction of genes with similar tissue-wide expression profiles and prediction of TF targets. (**A**) An overview of the machine learning framework. The steps enclosed in the dashed rectangle vary across prediction of genes with similar tissue-wide expression profiles and TF targets. The step with a dash-dotted border that intersects promoters with DHSs is a variant of the primary approach. In the IDBC algorithm (Additional file 1[21]), the parameter *I* is the minimum threshold on the total information contents of TFBS clusters. In prediction of genes with similar tissue-wide expression profiles, the minimum value was 939, which was the sum of mean information contents ($R_{sequence}$ values) of all 94 iPWMs; in prediction of direct targets, this value was the $R_{sequence}$ value of the single iPWM used to detect TFBSs. The parameter *d* is the radius of initial clusters in base pairs, whose value, 25, was determined empirically. The performance of seven different classifiers were evaluated with statistics (accuracy, sensitivity and specificity) (Additional file 1[21]). (**B**) Obtaining of the positives and negatives for identifying genes with similar tissue-wide expression profiles to a given gene (Additional file 2[21]). (**C**) Obtaining of the positives and negatives for predicting target genes of seven TFs using the CRISPR-generated perturbation data in K562 cells (Additional file 3[21]). (**D**) Obtaining of the positives and negatives for predicting target genes of 11 TFs using the siRNA-generated knockdown data in GM19238 cells (Additional file 4[21]).

The information density-related features (Additional file 1[21]) derived from each TFBS cluster included: 1) The distance between this cluster and the transcription start site (TSS); 2) The length of this cluster; 3) The information content of this cluster (i.e. the sum of R_i values of all TFBSs in this cluster); 4) The number of binding sites of each TF within this cluster; 5) The number of strong binding sites ($R_i > R_{sequence}$) of each TF within this cluster; 6) The sum of R_i values of binding sites of each TF within this cluster; 7) The sum of R_i values of strong binding sites ($R_i > R_{sequence}$) of each TF within this cluster.

For a gene, each of Features 1-3 was defined as a vector whose size equals the number of clusters in the promoter; thus, the entire vector could be input into a classifier. If two genes contained different numbers of clusters, the maximum number of clusters among all instances was determined, and null clusters were added at the 5' end of promoters with fewer clusters, enabling all instances to have the same cluster count. Using all instances as training data, machine learning classifiers with default parameter values in MATLAB were used to generate ROC curves (Additional file 1[21]).

Prediction of TF targets

Using gene expression in the CRISPR-based perturbations. Dixit *et al*. performed CRISPR-based perturbation experiments using multiple guide RNAs for each of ten TFs in K562 cells, resulting in a regulatory matrix of coefficients that indicate the effect of each guide RNA on each of 22,046 genes[15]. Data are available on Zenodo[20]. The coefficient of a guide RNA on a gene is defined as the $\log_{10}$(fold change in gene expression level)[15]. Among these ten TFs, we have previously derived iPWMs exhibiting primary binding motifs for seven (EGR1, ELF1, ELK1, ETS1, GABPA, IRF1, YY1)[3]. Therefore, the framework for predicting TF targets in the K562 cell line (Figure 1A and 1C) was applied to these TFs. The criteria for defining a positive (i.e. a target gene), of a TF were:

1) The fold change in the expression level of this gene for each guide RNA of the TF exceeds (or is less than) 1, eliminating those genes exhibiting both increased and decreased expression levels for different guide RNAs, and maximizing the possibility that the gene was downregulated (or upregulated) by the TF (Additional file 1[21]). and

2) The average fold change in the expression level of this gene for all guide RNAs of the TF exceeds the threshold ε (or is less than $1/\varepsilon$), and

3) The promoter interval (10 kb) upstream of a TSS of this gene overlaps a ChIP-seq peak of the TF in the K562 cell line.

If the coefficients of all guide RNAs of the TF for a gene are zero, the gene was defined as a negative. As the threshold ε increases, the number of positives strictly decreases; as ε decreases, we have increasingly lower confidence in the fact that the positives were indeed differentially expressed because of the TF perturbation. To achieve a balance, we evaluated three different values (i.e. 1.01, 1.05 and 1.1) for ε (Additional file 1[21]). For each TF, all ENCODE ChIP-seq peak datasets from the K562 cell line were merged to determine positives. Data are available on Zenodo[20]. To make the numbers of negatives and positives equal to avoid imbalanced datasets that significantly compromise the classifier performance[26], the Bray-Curtis function was applied to compute the similarity values in the tissue-wide expression profile between all negatives and the positive with the largest average coefficient, then the negatives with the smallest values were selected (Figure 1C).

The DHSs in the K562 cell line were intersected with known promoters. Data are available on Zenodo[20]. Because TFs may exhibit tissue-specific sequence preferences due to different sets of target genes and binding sites in different tissues[3], the iPWMs of EGR1, ELK1, ELF1, GABPA, IRF1, YY1 from the K562 cell line were used to most accurately detect binding sites; for ETS1, we used the only available iPWM from the GM12878 cell line[3]. Six features (Features 1-5 and 7) were derived from each homotypic cluster (i.e. Feature 6 became identical to Feature 3, because only binding sites from a single TF were used) (Figure 1A). The results of 10 rounds of 10-fold cross validation were averaged to more accurately evaluate the predictive power of the classifier.

Using gene expression in the siRNA-based knockdown. In the GM19238 cell line, 59 TFs were individually knocked down using siRNAs, and significant changes in the expression levels of 8,872 genes were indicated according to their corresponding P-values[13]. Data are available on Zenodo[20]. In these cases, the P-value of a gene for a TF is the probability of observing the change in the expression level of this gene under the null hypothesis of no differential expression after TF knockdown; thus, the larger the change in the expression level, the smaller the P-value and the more likely this gene is differentially expressed. They also indicated whether the promoters of these genes display evidence of binding to TFs by intersecting with ChIP-seq peaks in the GM12838 cell line. Among these 59 TFs, we have previously derived accurate iPWMs exhibiting primary binding motifs for 11 (BATF, JUND, NFE2L1, PAX5, POU2F2, RELA, RXRA, SP1, TCF12, USF1, YY1)[3]. Therefore, the framework for predicting TF targets in the GM19238 cell line (Figure 1A, D) was applied to these 11 TFs.

We defined a positive (i.e. a target gene) for a TF, if the P-value of this gene for the TF was ≤ 0.01, and the promoter interval (10 kb) upstream of a TSS of this gene overlapped a ChIP-seq peak of the TF in the GM12878 cell line. All other genes with P-values > 0.01 were considered to exhibit insufficient evidence of being TF targets, i.e. these were considered negatives or non-targets.

The DHSs in the GM19238 cell line mapped from the hg19 genome assembly were first remapped to the hg38 assembly using liftOver prior to being intersected with known promoters[27]. Data are available on Zenodo[20]. Aside from RELA, RXRA and NFE2L1, the iPWMs of TFs from the GM12878 cell line were used to detect binding sites. For RELA, the iPWM from the GM19099 cell line was used; for RXRA and NFE2L1, the only available iPWMs were respectively derived from HepG2 and K562 cells and were applied. Although the knockdown was performed in GM19238, GM12878 and GM19099 are also lymphoblastic cell lines, with GM19099 and GM19238 both being derived from Yorubans. For this analysis, the iPWMs derived in GM12878 and GM19099 were more appropriate sources of accessible TFBSs than those from HepG2 and K562, since GM12878 and GM19099 are of the same tissue type and are thus more likely comparable to GM19238 than HepG2 and K562. Similarly, the results of 10 rounds of 10-fold cross validation were averaged to more accurately evaluate the predictive power of the classifier.

Mutation analyses on promoters of TF targets

To better understand the significance of individual binding sites for information-dense clusters and the regulatory state of direct targets, we evaluated the effects of sequence changes that altered the R_i values of these sites on cluster formation and whether a gene was predicted to be a TF target. Mutations were sequentially introduced into the strongest binding sites in TFBS clusters of the EGR1 target gene, *MCM7*, to determine the threshold for cluster formation after disappearing clusters disabled induction of *MCM7* expression. For one target gene of each TF from the CRISPR-generated perturbation data, effects of naturally occurring TFBS variants present in dbSNP[28] were also evaluated to explore aspects of TFBS organization that enabled both clusters and promoter activity to be resilient to binding site mutations. This was done by analyzing whether the occurrence of individual or multiple single nucleotide polymorphisms (SNPs) lead to the loss of binding sites and the corresponding clusters, and resulted in changes in the predictions for these targets.

Results

Similarity between GTEx tissue-wide expression profiles of genes

To confirm that the Bray-Curtis Similarity can indeed effectively measure how akin the tissue-wide expression profiles of two genes are to one another, Equation 2 was applied to compute the similarity values between the tissue-wide expression profiles of the glucocorticoid receptor (*GR* or *NR3C1*) gene and all other 18,812 PC genes. NR3C1 is an extensively characterized TF with many known direct target genes[29]. As a constitutively expressed TF activated by glucocorticoid ligands, the protein can mediate the up-regulation of anti-inflammatory genes by binding of homodimers to glucocorticoid response elements and down-regulation of proinflammatory genes by complexing with other activating TFs (e.g. NFKB and AP1) and eliminating their ability to bind targets[29]. NR3C1 can bind its own promoter forming an auto-regulatory loop, which also contains functional

binding sites of 11 other TFs (e.g. SP1, YY1, IRF1, NFKB) whose iPWMs have been developed and/or mutual interactions have been described previously[3,29]. However, since the tissue-wide expression profile of *NR3C1* comprises all different splicing and translational isoforms (e.g. *GRα-A* to *GRα-D*, *GRβ*, *GRγ*, *GRδ*), the tissue-specific expression patterns of these isoforms are indistinguishable (e.g. levels of the *GRα-C* isoforms are significantly higher in the pancreas and colon, whereas levels of *GRα-D* are highest in spleen and lungs)[29]. *SLC25A32* and *TANK* have the greatest similarity in expression to *NR3C1* (0.880 and 0.877 respectively), which is evident based on their overall similar expression patterns across the 53 tissues (Figure 2).

Prediction of genes with similar GTEx tissue-wide expression profiles

In prediction of genes with similar tissue-wide expression profiles to *NR3C1*, we generated ROC curves to compare the performance of different classifiers (Naïve Bayes, Decision Tree (DT), Random Forest and Support Vector Machines (SVM) with four different kernels), under two scenarios depending on whether promoter sequences were first intersected with DHSs (Figure 3). DT exhibited the largest AUC (area under the curve) under both scenarios, and was one of two most stable classifiers (i.e. $\Delta AUC < 0.01$), with the other being the SVM with RBF kernel. Inclusion of DHS information significantly improved AUC values of the other classifiers with the exception of Naïve Bayes, and in many instances, all TFBSs in a contiguous DHS interval formed a single binding site cluster.

Prediction of TF targets

Since the DT classifier performed the best in distinguishing genes with *NR3C1*-like tissue-wide expression profiles from others, we further used this classifier type to predict TF targets respectively based on the CRISPR-[15] and siRNA-generated[13] perturbation data, and assessed its performance with 10 rounds of 10-fold cross validation. To validate that using all six machine learning features more comprehensively capture the distribution and composition of CRMs in the promoter, all of the features, except for TFBS counts, were removed. The classifier performance decreased, except for CRISPR-perturbed GABPA, IRF1 and YY1 after inclusion of DHS information (Additional file 5[21]).

On the CRISPR-generated knockdown data, after eliminating TFBSs in inaccessible promoter intervals, i.e. those excluded from tissue-specific DHSs, the DT classifier predicted TF targets with greater sensitivity and specificity (Table 3). Specifically, predictions for TFs: EGR1, ELK1, ELF1, ETS1, GABPA, and IRF1 were more accurate than for YY1, which itself represses or activates a wide range of promoters by binding to sites overlapping the TSS (Table 3). Accordingly, the perturbation data indicated that YY1 has ~4-22 times more PC targets in the K562 cell line than the other TFs ($\varepsilon = 1.05$), and its binding has a more significant impact on the expression levels of target genes (for YY1, the ratio of the PC target counts at $\varepsilon = 1.1$ vs $\varepsilon = 1.01$ was 0.334, which significantly exceeded those of the other TFs (0.017-0.082); Additional file 3[21]). This is concordant with our previous finding that YY1 extensively interacts with 11 cofactors (e.g. DNA-binding IRF9 and TEAD2; non-DNA-binding DDX20 and PYGO2) in K562 cells, consistent with a central role in specifying erythroid-specific lineage development[3].

Despite a high accuracy of target recognition, sensitivity did not exceed specificity except for IRF1 (Table 3), due to a relatively large number of false negative genes. We find that promoters of most TF targets contain accessible, likely functional binding sites that significantly are correlated with changes in gene expression levels. By contrast, promoters of non-targets contain either no accessible binding sites at all, or accessible, but non-functional sites. The fact that these false negatives were erroneously predicted to non-targets was attributable to the inability of the classifier to distinguish between likely functional binding sites in their promoters and non-functional ones in non-targets in some cases. *In vivo* co-regulation mediated by interacting cofactors, which was excluded by the classifier, assisted in distinguishing these non-functional sites that do not significantly affect gene expression[13].

As the threshold ε increased, the accuracy of the classifier for all the TFs monotonically increased as expected (Figure 4). For a gene to be defined as a DE target of a TF, the average fold change in its expression level for all guide RNAs that downregulated the TF were required to reach the minimum threshold ε. Upon TF knockdown, ε is inversely correlated with the number of target genes, but positively correlated with fold changes in their corresponding expression levels. In general, more significantly DE genes have been associated with a higher number of TFBSs in their promoters[13]. Thus, at greater ε, there are larger differences in the values of machine learning features derived from TFBS clusters between direct targets and non-targets.

With the siRNA-generated knockdown data, the performance of the DT classifier was compared to the approach inferring DE targets by correlating TF binding with gene expression levels across ten cell types[14]. In this correlation-based approach, three measures (i.e. the absolute Pearson correlation coefficient (PCC), the absolute Spearman correlation coefficient (SCC), and the absolute combined angle ratio statistic (CARS)), whose performance was evaluated with precision-recall curves, were alternatively used to compute a correlation score between the number of ChIP-seq peaks overlapping the promoter and gene expression values. Genes predicted to be DE targets had scores above the threshold resulting in a 1.5-fold increase compared to the background precision (i.e. the DE target count / 8,872). For example, in the case of YY1, which was the only TF analyzed by both approaches, the performance of the DT classifier was 0.98 (precision) and 0.55 (recall) after including DHS information (Table 4). This classifier outperformed all three correlation measures (PCC: 0.467 and 0.003; SCC: 0.467 and 0.006; CARS: 0.467 and 0.003 directly obtained from 14), even though the correlation-based approach used a less stringent P-value threshold (0.05) for defining differential expression of likely non-direct targets, and intersected ChIP-seq peaks over shorter 5kb promoter intervals upstream of the TSS. Three reasons explain why the correlation-based approach exhibited lower recall, including: 1) it did not use machine learning classifiers, 2) its

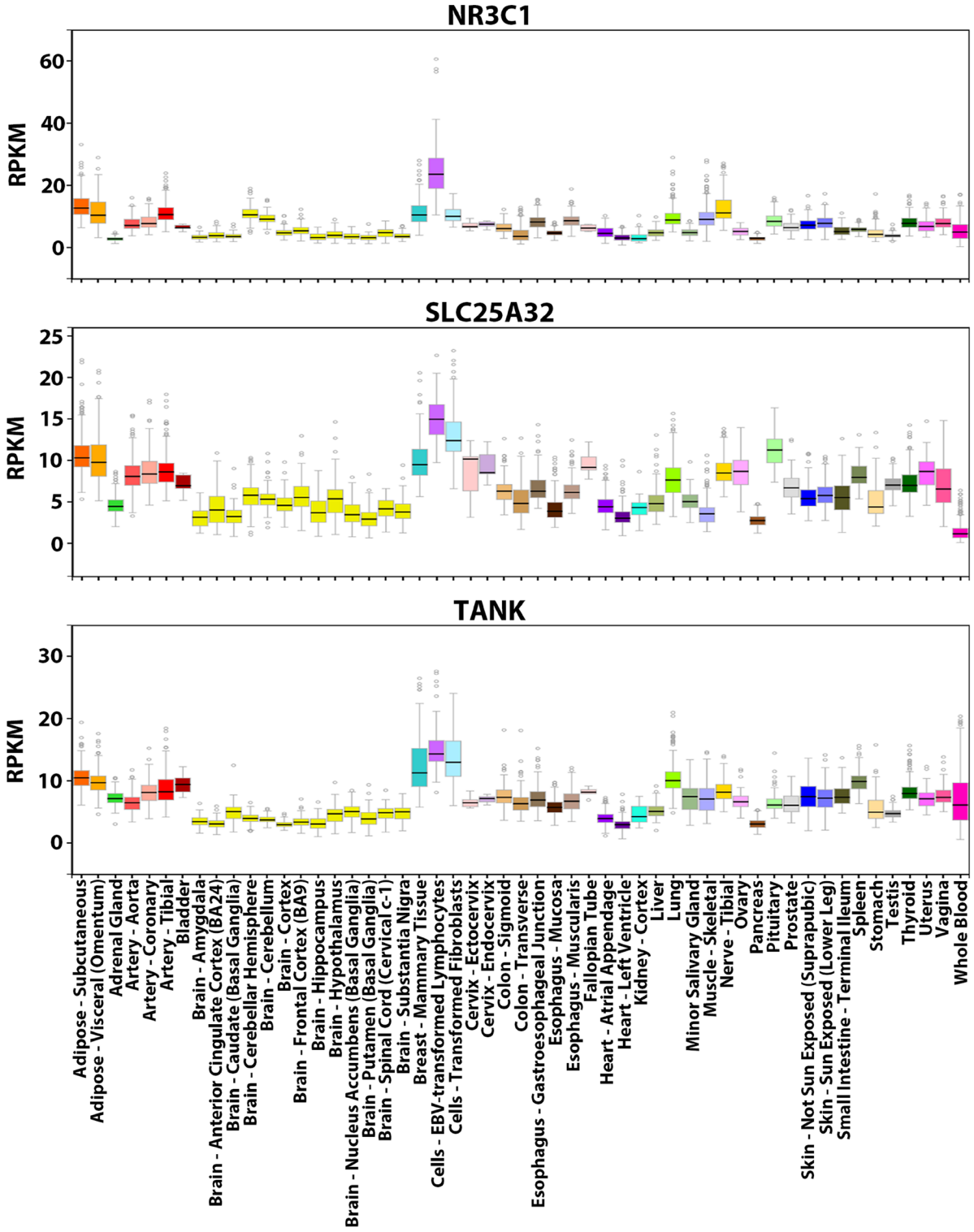

Figure 2. GTEx tissue-wide expression profiles of *NR3C1*, *SLC25A32* and *TANK*. Visualization of the expression values (in RPKM) of these genes across 53 tissues from GTEx. For each gene, the colored rectangle belonging to each tissue indicates the valid RPKM of all samples in the tissue, the black horizontal bar in the rectangle indicates the median RPKM, the hollow circles indicate the RPKM of the samples considered as outliers, and the grey vertical bar indicates the sampling error. By comparing the pictures, the overall expression patterns of the three genes across the 53 tissues resemble each other (e.g. all three genes exhibit the highest expression levels in lymphocytes and the lowest levels in brain tissues).

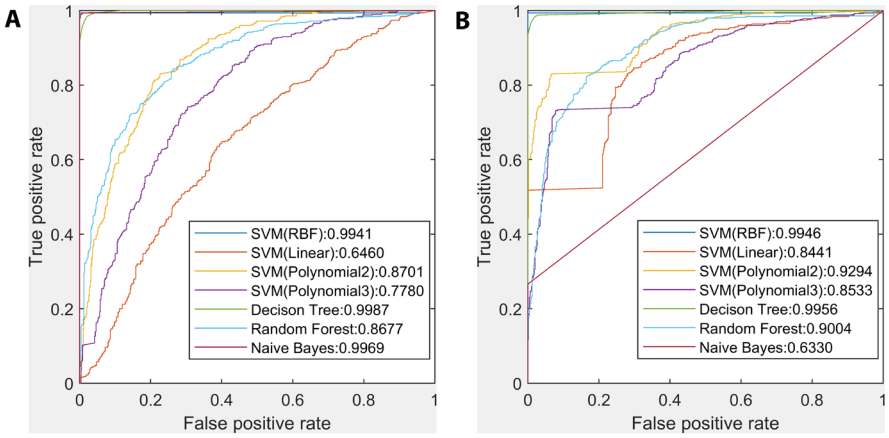

Figure 3. Comparison between the performance of different classifiers in prediction of genes with similar tissue-wide expression profiles to *NR3C1*. (**A**) ROC curves and AUC of seven classifiers without intersecting promoters with DHSs. (**B**) ROC curves and AUC of seven classifiers after intersecting promoters with DHSs. The Decision Tree classifier exhibited the largest AUC under both scenarios, and inclusion of DHS information significantly improved other classifiers' AUC except for Naïve Bayes.

Table 3. The Decision Tree classifier performance for predicting TF targets using the CRISPR-generated knockdown data.

TF	Excluding DHS information†			Including DHS information†		
	Sensitivity	Specificity	Accuracy	Sensitivity	Specificity	Accuracy
EGR1	0.58	0.62	0.60	0.78	0.81	0.80
ELF1	0.59	0.65	0.62	0.83	0.87	0.85
ELK1	0.59	0.59	0.59	0.80	0.81	0.81
ETS1	0.59	0.6	0.59	0.81	0.81	0.81
GABPA	0.55	0.57	0.56	0.72	0.75	0.74
IRF1	0.54	0.55	0.54	0.76	0.64	0.70
YY1	0.50	0.51	0.51	0.45	0.69	0.57

†The average performance of 10 rounds of 10-fold cross validation when setting ε to 1.05 is indicated. The CRISPR-generated knockdown data were obtained from Dixit *et al.*[15].

larger P-value threshold (0.05) generated a larger number of positives and, 3) positives also include DE targets that cannot be directly bound.

Intersection of genes with similar tissue-wide expression profiles and TF targets

To determine how many TF targets have similar tissue-wide expression profiles, we intersected the set of targets with the set of 500 PC genes with the most similar tissue-wide expression profiles for each TF (Table 5, Additional file 6[21]). The TFs PAX5 and POU2F2 are primarily expressed in B cells, and their respective targets *IL21R* and *CD86* are also B cell-specific, which accounts for the high similarity in the tissue-wide expression profile between them. There are respectively 21 and 7 nuclear mitochondrial genes (e.g. *MRPL9* and *MRPS10*, which are subunits of mitochondrial ribosomes) in the intersections for YY1 in the K562 and GM19238 cell lines[30]. Previous studies reported that YY1 upregulates a large number of mitochondrial genes by complexing with PGC-1α in C2C12 cells[31], and genes involved in the mitochondrial respiratory chain in K562 cells[15], which is consistent with the idea that YY1 may broadly regulate mitochondrial function (within all 53 tissues in addition to the erythrocyte, lymphocyte and skeletal muscle cell lines).

Between 0.4%–25% of genes with similar tissue-wide expression profiles to the TFs are actually their targets (Table 5); the majority are non-targets whose promoters contain non-functional binding sites that are distinguished from targets by their lack of co-regulation by corresponding cofactors. For YY1 and EGR1, we validated this hypothesis by contrasting the flanking cofactor binding site distributions and strengths in the promoters of the most similarly expressed target genes (YY1: *MRPL9*, *BAZ1B*; EGR1: *CANX*, *NPM1*) and non-target genes (YY1: *ADNP*, *RNF25*; EGR1: *GUCY2F*, *AWAT1*). In the promoters of these target genes, strong and intermediate recognition sites for TFs: SP1, KLF1, CEBPB formed heterotypic clusters with adjacent

YY1 sites; as well TFBSs of SP1, KLF1, and NFY were frequently present adjacent to EGR1 binding sites (Additional file 7[21]). These patterns contrasted with the enrichment of CTCF and ETV6 binding sites in gene promoters of *YY1* and *EGR1* non-targets (Additional file 7[21]). Previous studies have reported that KLF1 is essential for terminal erythroid differentiation and maturation[32], direct physical interactions between YY1 and the constitutive activator SP1 synergistically induce transcription[33], the activating CEBPB promotes differentiation and suppresses proliferation of K562 cells by binding the promoter of the *G-CSFR* gene encoding a hematopoietin receptor[34], EGR1 and SP1 synergistically cooperate at adjacent non-overlapping sites on *EGR1* promoter but compete binding at overlapping sites[35]; whereas occupied CTCF binding sites often function as an insulator blocking the effects of *cis*-acting elements and preventing gene activation by mediating long-range DNA loops to alter topological chromatin structure[36,37], and ETV6, a member of the ETS family, is a transcriptional repressor required for bone marrow hematopoiesis and associated with leukemia development[38].

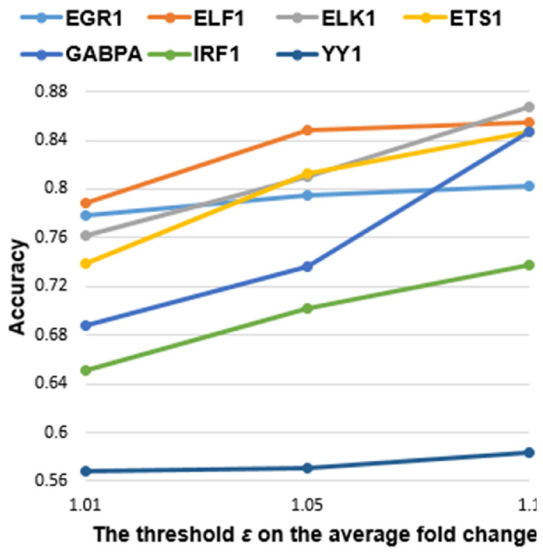

Figure 4. Accuracy of the Decision Tree classifier when using three different values for ε. Each accuracy value was averaged from 10 rounds of 10-fold cross validation, when the minimum threshold ε on the average fold change in gene expression levels under all guide RNAs of the TF took three different values 1.01, 1.05 and 1.1. As ε increased, accuracy for all seven TFs monotonically increased.

Mutation analyses on promoters of direct targets

Because the promoters of direct target genes contain multiple binding site clusters, we hypothesized that this organization could stabilize gene expression against the effect of mutations in individual binding sites; in other words, the other clusters might be able to compensate for the loss of a cluster destroyed by mutations, so that the mutated promoters would still be capable of effectively regulating gene transcription upon TF binding. First, we examined whether introducing artificial variants into binding sites *in silico* in the promoter of the target gene *MCM7* of EGR1 changed the classifier output (Figure 5). Specifically, in the K562 cell line, *MCM7* is upregulated by EGR1. Knockdown of *MCM7* has an anti-proliferative and pro-apoptotic effect on K562 cells[39] and the loss of EGR1 increases leukemia initiating cells[40], which suggests that EGR1 may act as a tumor suppressor in K562 cells through the *MCM7* pathway.

First, the strongest binding site (at position chr7:100103347[hg38], - strand, R_i = 12.0 bits) in the promoter was eliminated by a G->A mutation, resulting in the loss of Cluster 1, which

Table 4. The Decision Tree classifier performance for predicting TF targets using the siRNA-generated knockdown data.

TF	Excluding DHS information†			Including DHS information†		
	Sensitivity	Specificity	Accuracy	Sensitivity	Specificity	Accuracy
BATF	0.96	0.97	0.96	0.85	1	0.93
JUND	0.86	0.90	0.88	0.80	1	0.90
NFE2L1	0.92	0.95	0.94	0.71	0.93	0.82
PAX5	0.96	0.97	0.96	0.88	0.98	0.93
POU2F2	0.97	0.97	0.97	0.89	0.99	0.94
RELA	0.95	0.96	0.96	0.83	0.97	0.90
RXRA	0.93	0.91	0.92	0.84	0.95	0.89
SP1	0.98	0.98	0.98	0.89	0.99	0.94
TCF12	0.98	0.98	0.98	0.86	0.99	0.93
USF1	0.97	0.98	0.97	0.83	0.98	0.90
YY1	1	1	1	0.55	0.99	0.77

†The average performance of 10 rounds of 10-fold cross validation is indicated. The siRNA-generated knockdown data were obtained from Cusanovich *et al.*[13].

Table 5. Intersection of TF targets and 500 protein-coding genes with the most similar tissue-wide expression profiles.

TF	Cell line	Number of targets	Size of intersection	Targets among the most similar 10 genes§
EGR1	K562	169	12	None
ELF1		78	5	None
ELK1		112	4	*GNL1*(8th)
ETS1		267	15	None
GABPA		513	25	TAF1(1st)
IRF1		457	10	None
YY1		1752	127	*MRPL9*(2nd), *BAZ1B*(6th), *ENY2*(7th), *NUB1*(8th), *USP1*(9th), *HNRNPR*(10th)
	GM19238	1040	61	*MED4*(1st), *SURF6*(3rd), *BAZ1B*(6th)
BATF		186	21	None
JUND		44	2	None
NFE2L1		58	4	None
RELA		247	13	*HMG20B*(9th)
RXRA		181	3	None
SP1		1595	81	None
TCF12		655	20	None
USF1		301	21	None
PAX5		918	86	*IL21R*(8th)
POU2F2		532	26	*CD86*(3rd)

§The rank of each target in the list of similar genes in the descending order of Bray-Curtis similarity values is shown in the brackets immediately following the target.

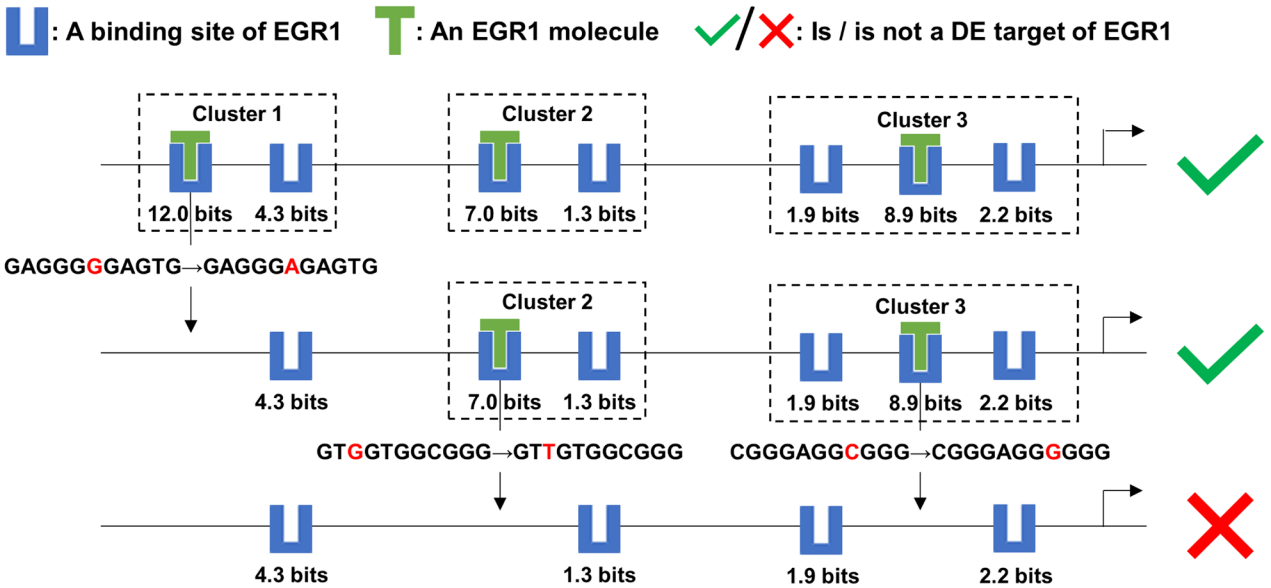

Figure 5. Mutation analyses on the target *MCM7* of EGR1. This figure depicts the effect of a mutation in each EGR1 binding site cluster of the *MCM7* promoter on the expression level of *MCM7*, which is a target of the TF EGR1. The strongest binding site in each cluster were abolished by a single nucleotide variant. Upon loss of all three clusters, only weak binding sites remained and EGR1 was predicted to no longer be able to effectively regulate *MCM7* expression. Multiple clusters in the promoters of TF targets confer robustness against mutations within individual binding sites that define these clusters.

consists of two sites (the other site at chr7:100103339, -, 4.3 bits). The other two clusters comprising weaker binding sites of intermediate strength (chr7:100102252, +, 7.0 bits; chr7:100102244, +, 1.3 bits; chr7:100101980, +, 8.9 bits; chr7:100101977, +, 2.2 bits; chr7:100101984, +, 1.9 bits) were still predicted to compensate for this mutation, enabling the promoter to maintain capability of inducing *MCM7* expression (Figure 5). It is well known that adjacent clustered sites, which themselves may not be strong enough to individually bind TFs and activate transcription, can stabilize each other's binding[2]. The weaker sites flanking a strong binding site in a cluster can direct the TF molecule to the strong site and extend the period of the molecule physically associating with the strong site, which is termed, the funnel effect[2]. In this example, Clusters 2 and Cluster 3 were also respectively removed by G->T and C->G mutations abolishing the strongest site in either cluster, which altered the prediction, that is, EGR1 should lose the capability to induce *MCM7* transcription (Figure 5). The remaining four sparse weak sites do not form a cluster and cannot completely supplant the disrupted strong sites.

Further, we examined the predicted impacts of known natural SNPs on binding site strengths, clusters and the regulatory state of the promoter for a direct target of each of the seven TFs from the CRISPR-generated perturbation data (Table 6). Often a single SNP (e.g. rs996639427 of EGR1) can affect the strengths of multiple binding sites (Table 6). Apart from SNPs that are predicted to abolish binding (Figure 5), leaky variants that merely weaken TF binding are common (Table 6). Binding stabilization between adjacent sites and the funnel effect enable CRMs comprised of information-dense clusters to be robust to mutations in individual binding sites[2,41]. In this way, neither mutations that abolish TFBSs nor leaky SNPs in flanking weak sites would be expected to destroy clusters (e.g. rs1030185383 and rs5874306 of IRF1), whereas SNPs with large reductions in R_i values of central strong sites are more likely to abolish clusters (e.g. rs865922947, rs946037930, rs917218063 and rs928017336 of YY1) (Table 6). More generally, the presence of multiple clusters enables promoters to be effectively resilient to the effects of binding site mutations; only the complete abolishment of all clusters resulting from the simultaneous occurrence of multiple SNPs should be able to transform the promoter to be unresponsive to TF binding to residual weak sites (e.g. rs997328042, rs1020720126 and rs185306857 of GABPA) (Table 6). Furthermore, a relatively small number of SNPs that strengthen TF binding and eventually reinforce the regulatory effect of the TF are also present in these cases (e.g. rs887888062 of EGR1 and rs751263172 of ELF1) (Table 6), suggesting that, in addition to deleterious mutations, potentially benign variants may also be found in promoters, consistent with the expectations of neutral theory[42].

Discussion

In this study, the Bray-Curtis similarity function was initially shown (for the *NR3C1* gene) to measure the relatedness of overall expression patterns between genes across a diverse set of tissues. A machine learning framework distinguished Bray-Curtis function-defined similar from dissimilar genes based on the distribution, strengths and compositions of TFBS clusters in accessible promoters, which can substantially account for the corresponding gene expression patterns. Using knockdown data as the gold standard, the combinatorial use of TF binding profiles and chromatin accessibility was also demonstrated to be predictive of TF targets. A binding site comparison confirmed that coregulatory cofactors can be used to distinguish between functional sites in targets and non-functional ones in non-targets. Furthermore, mutation analyses on binding sites of targets demonstrated that the existence of both multiple TFBSs in a cluster and multiple information-dense clusters in a promoter enables both the cluster and the promoter to be resilient to binding site mutations.

The DT classifier improved after intersecting promoters with DHSs in prediction of TF targets with the CRISPR-generated knockdown data (Table 3). This intersection eliminated noisy binding sites that are inaccessible to TF proteins in promoters; specifically, it widened discrepancies in feature vectors between positives and negatives. If the 10 kb promoter of a gene instance does not overlap DHSs, its feature vector will only consist of 0; the percentages of negatives whose promoters do not overlap DHSs considerably exceeded those of positives (Additional file 8[21]), which led to an excess of negatives with feature vectors containing only 0 after intersection. This explains why these negatives are not DE targets of the TFs in the K562 and GM19238 cell lines, because their entire promoters are not open to TF molecules; other regulatory regions besides the proximal promoters (e.g. intronic enhancers[43]) still enable the TFs to effectively control the expression of the positives with inaccessible promoters. The relatively poor performance of the classifier on YY1 (Table 3) is attributable to its smaller percentage of negatives with inaccessible promoters (Additional file 8[21]) and the larger number of functional binding sites in the K562 cell line.

Our *in-silico* mutation analyses revealed that some deleterious TFBS mutations could be compensated for by other information-dense clusters in the same promoter[2]; thus, predicting the effects of mutations in individual binding sites might not be sufficient to interpret downstream effects without considering their context. Though compensatory clusters may maintain gene expression, the promoter will provide lower levels of activity than the wild-type promoter could, which is a recipe for achieving natural phenotypic diversity[41]. Few published studies in molecular diagnostics have specifically examined the effects of naturally occurring variants within clustered TFBSs; thus, IDBC-based machine learning provides an alternative computational approach to predict deleterious mutations that actually impact (i.e. repress or abolish) transcription of target genes and result in abnormal phenotypes, and to simultaneously minimize false positive calls of TFBS mutations that individually have little or no impact.

Apart from these TFs, the Bray-Curtis Similarity can be directly applied to identify the ground-truth genes with overall similar tissue-wide expression patterns to any other gene whose expression profile is known. Further studies could investigate the biological significance underlying the phenomenon that all these genes share a common expression pattern, including the

Table 6. Mutation analyses on promoters of TF targets.

TF	Target	Normal cluster	Normal binding site[§]	SNP ID[§]	Variant binding site[§]	Variant cluster[‡]	Classifier output		
							Variant[†]		Wild-type
EGR1 ($R_{sequence}$ = 12.2899 bits)	*EID2B*	Cluster 1 of 2	**G**A**G**GGGGC**AT**C (chr19:39540296, -, 7.22 bits)	rs538610162 (chr19:39540296C>G)	**C**AGGGGGCATC (chr19:39540286, -, 4.84 bits)	Abolished	√		√
				rs759233998 (chr19:39540294C>T)	GA**A**GGGGCATC (chr19:39540286, -, 0.06 bit)	Abolished	√		
				rs974735901 (chr19:39540288T>A)	GAGGGGGC**T**TC (chr19:39540286, -, 6.90 bits)	Cluster 1 of 2	√		
				rs978230260 (chr19:39540287A>T)	GAGGGGGCA**A**C (chr19:39540286, -, 5.31 bits)	Abolished	√		
		Cluster 2 of 2	**G**CGTGCGT**G**GG (chr19:39540162, +, 1.59 bits)	rs764734511 (chr19:39540162G>A) (chr19:39540162G>C)	**A**CGTGCGTGGG (chr19:39540162, +, -0.72 bit)	Cluster 2 of 2	√	×	
					CCGTGCGTGGG (chr19:39540162, +, -0.79 bit)	Cluster 2 of 2	√		
				rs996639427 (chr19:39540170G>C)	GCGTGCGT**C**GG (chr19:39540162, +, -5.21 bits)	Abolished	√		
					GCGT**C**GGCGCT (chr19:39540165, +, -0.85 bit)				
			GCGT**G**GGC**G**C**T** (chr19:39540166, +, 9.72 bits)	rs1027751538 (chr19:39540174G>A)	GCGTGGGC**A**CT (chr19:39540166, +, 5.16 bits)	Abolished	√		
				rs887888062 (chr19:39540176T>A)	GCGTGGGCGC**A** (chr19:39540166, +, 10.94 bits)	Cluster 2 of 2	√		
ELF1 ($R_{sequence}$ = 11.2057 bits)	*HIST1H4H*	Cluster 1 of 2	GC**GGA**AG**CG**TG (chr6:26286540, +, 9.92 bits)	rs760968937 (chr6:26286547C>T) (chr6:26286547C>A)	GCGGAAG**T**GTG (chr6:26286540, +, 10.71 bits)	Cluster 1 of 2	√	√	√
					GCGGAAG**A**GTG (chr6:26286540, +, 8.84 bits)	Cluster 1 of 2	√	×	
				rs1000196206 (chr6:26286542G>C)	GC**C**GAAGCGTG (chr6:26286540, +, -6.26 bits)	Abolished	√		
				rs144759258 (chr6:26286543G>A)	GCG**A**AAGCGTG (chr6:26286540, +, -3.60 bits)	Abolished	√		
				rs966435996 (chr6:26286544A>G)	GCGG**G**AGCGTG (chr6:26286540, +, 5.28 bits)	Abolished	√		
				rs950986427 (chr6:26286548G>A)	GCGGAAGC**A**TG (chr6:26286540, +, 8.28 bits)	Cluster 1 of 2	√		
		Cluster 2 of 2	**C**AG**GAG**ATGC**G** (chr6:26286483, -, 6.98 bits)	rs373649904 (chr6:26286483G>A)	**T**AGGAGATGCG (chr6:26286473, -, 0.61 bit)	Abolished	√		
				rs926919149 (chr6:26286480C>T)	CAG**A**AGATGCG (chr6:26286473, -, -6.53 bits)	Abolished	√		
				rs751263172 (chr6:26286479T>G)	CAGG**C**GATGCG (chr6:26286473, -, 1.24 bits)	Abolished	√		
				rs369076253 (chr6:26286473C>G)	CAGGAGATGC**C** (chr6:26286473, -, 6.92 bits)	Cluster 2 of 2	√		
				rs751263172 (chr6:1044474314C>T)	CAGGA**A**ATGCG (chr6:26286473, -, 11.43 bits)	Cluster 2 of 2	√	√	

TF	Target	Normal cluster	Normal binding site[§]	SNP ID[§]	Variant binding site[§]	Variant cluster[‡]	Classifier output		
							Variant[†]		Wild-type
ELK1 ($R_{sequence}$ = 11.9041 bits)	*G0S2*	Cluster 1 of 2	C***AG***GGAAG***A***CC (chr1:209667969, -, 1.92 bits)	rs146048477 (chr1:209667961T>A)	CAGGGAAG***T***CC (chr1:209667959, -, 2.24 bits)	Cluster 1 of 2	√	√	√
				rs887606802 (chr1:209667968T>C)	C***G***GGGAAGACC (chr1:209667959, -, -3.35 bits)	Cluster 1 of 2	√	×	
				rs1021034916 (chr1:209667967C>T)	CA***A***GGAAGACC (chr1:209667959, -, -3.57 bits)	Cluster 1 of 2	√		
			GAGGA***A***ATGAG (chr1:209667969, +, 8.14 bits)	rs941962117 (chr1:209667974A>G)	GAGGA***G***ATGAG (chr1:209667969, +, 4.11 bits)	Abolished	√		
		Cluster 2 of 2	***C***TGGAAGA***GC***A (chr1:209673554, -, 5.91 bits)	rs896117033 (chr1:209673545G>A)	CTGGAAGAG***T***A (chr1:209673544, -, 3.95 bits)	Cluster 2 of 2	√		
				rs971962577 (chr1:209673546C>T)	CTGGAAGA***A***CA (chr1:209673544, -, 3.49 bits)	Cluster 2 of 2	√		
				rs1011969709 (chr1:209673554G>C)	***G***TGGAAGAGCA (chr1:209673544, -, 3.92 bits)	Abolished	√		
			CCA***G***AAGTCA***A*** (chr1:209673551, +, 7.44 bits)		CCA***C***AAGTCAA (chr1:209673551, +, -5.50 bits)				
				rs1023312090 (chr1:209673561A>G)	CCAGAAGTCA***G*** (chr1:209673551, +, 8.40 bits)	Cluster 2 of 2	√	√	
ETS1 ($R_{sequence}$ = 10.0788 bits)	*TTC19*	Cluster 1 of 1	GCA***G***GGAA***A***GG (chr17:16022293, +, 7.92 bits)	rs1022234223 (chr17:16022296G>C)	GCA***C***GGAAAGG (chr17:16022293, +, -4.98 bits)	Abolished	×	×	√
				rs968299415 (chr17:16022301A>T)	GCAGGGAA***T***GG (chr17:16022293, +, 10.01 bits)	Cluster 1 of 1	√	√	
GABPA ($R_{sequence}$ = 10.8567 bits)	*PLEKHB2*	Cluster 1 of 1	A***C***A***G***GAAAGGG (chr2:131112770, +, 10.36 bits)	rs997328042 (chr2:131112771C>T)	A***T***AGGAAAGGG (chr2:131112770, +, -3.68 bits)	Abolished	×	×	√
				rs1020720126 (chr2:131112773G>C)	ACA***C***GAAAGGG (chr2:131112770, +, -4.16 bits)	Abolished	×		
			T***CT***GGAAAC***T***A (chr2:131112760, +, 1.53 bits)	rs185306857 (chr2:131112761C>A)	T***A***TGGAAACTA (chr2:131112760, +, -2.86 bits)	Cluster 1 of 1	√		
				rs772728699 (chr2:131112762T>A)	TC***A***GGAAACTA (chr2:131112760, +, 5.23 bits)	Cluster 1 of 1	√		
				rs965753671 (chr2:131112769T>C)	TCTGGAAAC***C***A (chr2:131112760, +, 2.13 bits)	Cluster 1 of 1	√		

TF	Target	Normal cluster	Normal binding site[§]	SNP ID[§]	Variant binding site[§]	Variant cluster[‡]	Classifier output		
							Variant[†]		Wild-type
IRF1 ($R_{sequence}$ = 13.5544 bits)	*SMIM13*	Cluster 1 of 1	***GA***G***A***A***T***GAA***A***GC***A*** (chr6:11093663, +, 12.56 bits)	rs950528541 (chr6:11093663G>C)	***C***AGAATGAAAGCA (chr6:11093663, +, 8.97 bits)	Cluster 1 of 1	√		√
				rs886259573 (chr6:11093664A>G)	G***G***GAATGAAAGCA (chr6:11093663, +, 9.65 bits)	Cluster 1 of 1	√		
				rs982931728 (chr6:11093666A>G)	GAG***G***ATGAAAGCA (chr6:11093663, +, 8.09 bits)	Cluster 1 of 1	√		
				rs1020218811 (chr6:11093668T>G)	GAGAA***G***GAAAGCA (chr6:11093663, +, 9.36 bits)	Cluster 1 of 1	√		
				rs570723026 (chr6:11093672A>G)	GAGAATGAA***G***GCA (chr6:11093663, +, 8.01 bits)	Cluster 1 of 1	√	×	
				rs1004825794 (chr6:11093675A>C) (chr6:11093675A>T)	GAGAATGAAAGC***C*** (chr6:11093663, +, 10.47 bits)	Cluster 1 of 1	√		
					GAGAATGAAAGC***A*** (chr6:11093663, +, 10.42 bits)	Cluster 1 of 1	√		
			AA***G***ACCAA***AG***GCA (chr6:11093641, +, 2.43 bits)	rs1030185383 (chr6:11093649A>C)	AAGACCAA***C***GGCA (chr6:11093641, +, -3.39 bits)	Cluster 1 of 1	√		
				rs5874306 (chr6:11093650delG)	AAGACCAAAGCAG (chr6:11093641, +, 0.90 bit)	Cluster 1 of 1	√		
				<u>rs558896490 (chr6:11093643G>A)</u>	<u>AA***A***ACCAAAGGCA (chr6:11093641, +, 7.06 bits)</u>	Cluster 1 of 1	√	√	
YY1 ($R_{sequence}$ = 12.8554 bits)	*CKLF*	Cluster 1 of 1	***G***C***GG***C***C***ATCGGC (chr16:66549797, -, 10.06 bits)	rs865922947 (chr16:66549791G>A)	***C***CGGCCATCGGC (chr16:66549785, -, 6.80 bits)	Cluster 1	√		√
				rs946037930 (chr16:66549794C>A)	GC***T***GCCATCGGC (chr16:66549785, -, 8.02 bits)	Cluster 1	√		
				rs917218063 (chr16:66549793C>T)	GCG***A***CCATCGGC (chr16:66549785, -, 5.41 bits)	Abolished	×	×	
				rs928017336 (chr16:66549791G>A)	GCGGC***T***ATCGGC (chr16:66549785, -, -3.62 bits)	Abolished	×		
				GCCGCCCCCGTC (chr16:66549792, +, 1.34 bits)					

[§]All coordinates are based on the hg38 genome assembly. A bold italic letter in a binding site sequence indicates the base where a SNP occurs. For each normal and variant binding site sequence, the genome coordinate of its most 5'-end base and its R_i value are indicated. The negative R_i value of a variant binding site sequence implies this site is abolished. The SNPs strengthening binding sites and corresponding variant binding site sequences are underlined.

[‡]The impact on whether the occurrence of a single SNP resulted in the disappearance of the cluster containing it is shown; 'Abolished' indicates that the cluster is eliminated by the existence of the variant allele.

[†]After a single SNP occurred or multiple SNPs simultaneously occurred, the classifier produced a new prediction on whether the TF is still capable of significantly affecting gene expression via the variant promoter.

similarity between other regulatory regions besides proximal promoters in terms of TFBSs and epigenetic markers. This machine learning framework can also be applied to predict target genes for other TFs and in other cell lines, depending on the availability of corresponding knockdown data.

There are a number of limitations of our approach. The Bray-Curtis function seems unable to accurately measure the similarity between the tissue-wide expression profiles of a gene (e.g. *MIR23A*) without any detectable mRNA in any of the 53 tissues analyzed and genes (e.g. the ubiquitously expressed *NR3C1*

and stomach-specific *PGA3*) that are expressed in at least one tissue. Intuitively, in terms of expression patterns *PGA3* is more similar to *MIR23A* than *NR3C1*; however, the Bray-Curtis similarity values indicate that both *PGA3* and *NR3C1* bear no similarity to *MIR23A* (i.e. $sim_{Bray\text{-}Curtis}$ (*NR3C1*, *MIR23A*) = $sim_{Bray\text{-}Curtis}$ (*PGA3*, *MIR23A*) = 0). Another possible limitation in classifier performance in the prediction of genes with similar tissue-wide expression profiles is that only binding sites of 82 TFs were analyzed due to a lack of available iPWMs for other TFs, given that 2000-3000 sequence-specific DNA-binding TFs are estimated to be encoded in the human genome[44]. For example, four TFs (CREB, MYB, NF1, GRF1) were previously reported to bind the promoter of the *NR3C1* gene to activate or repress its expression; however, their iPWMs exhibiting known primary motifs could not be successfully derived from ChIP-seq data[3,29]. Regarding the CRISPR-generated knockdown data used here, positives were inferred to be direct targets by intersecting their promoters with corresponding ChIP-seq peaks, which may not be completely accurate, due to the presence of noise peaks that do not contain true TFBSs[3,45]. Small fold changes in the expression levels of DE targets could arise from compromised efficiency of knockdowns as a result of suboptimal guide RNAs or the limitations of perturbing only a single allele of the TF[46]. Finally, the framework developed here only takes into account the 10 kb interval proximal to the TSS, and would not therefore capture long range enhancer effects beyond this distance; by contrast, correlation based approaches have successfully incorporated multiple definitions of promoter length[14].

Conclusions

The Bray-Curtis function is able to effectively quantify the similarity between tissue-wide gene expression profiles. By analysis of information theory-based TF binding profiles that captured the spatial distribution and information contents of TFBS clusters, ChIP-seq and chromatin accessibility data, we described a machine learning framework that distinguished tissue-wide expression profiles of similar vs dissimilar genes and identified TF target genes. Functional binding sites in target genes that significantly alter expression levels upon direct binding are at least partially distinguished by TF-cofactor coregulation from non-functional sites in non-targets. Finally, *in-silico* mutation analyses demonstrated that the presence of multiple information-dense clusters in the promoter, as a protective mechanism, reduces deleterious mutations that can significantly alter the regulatory state and expression level of the gene.

An earlier version this article is available from bioRxiv: https://doi.org/10.1101/283267[47].

Data availability

Underlying data

The median RPKM, TSS coordinate, DNase I hypersensitivity and ChIP-seq data were respectively obtained from the GTEx Analysis V6p release (www.gtexportal.org), Ensembl Biomart (www.ensembl.org) and ENCODE (www.encodeproject.org). The CRISPR- and siRNA-generated knockdown data were obtained from the supplementary information files of Dixit *et al.*[15] and Cusanovich *et al.*[13]. The source datasets generated and/or analysed by this framework, along with sample results and compiled software are available from Zenodo. DOI: https://doi.org/10.5281/zenodo.1707423[20].

Extended data

Additional files are available from Zenodo. DOI: https://doi.org/10.5281/zenodo.1698281[21].

Additional file 1. The mathematical definitions of the four other similarity metrics, the workflow of the IDBC algorithm, an example feature vector, the mathematical definitions of five statistical variables to measure classifier performance, the default parameter values of classifiers in MATLAB, and histograms visualizing the first two criteria for selecting positives from the CRISPR-generated knockdown data.

Additional file 2: The lists of positives and negatives in the machine learning classifiers to predict genes with similar tissue-wide expression profiles.

Additional file 3: The lists of positives and negatives in the DT classifier to predict TF targets based on the CRISPR-generated knockdown data.

Additional file 4: The lists of positives and negatives in the DT classifier to predict DE direct targets based on the siRNA-generated knockdown data.

Additional file 5: The performance of the DT classifier using only TFBS counts.

Additional file 6: The list of the most similar 500 PC genes to each TF in terms of tissue-wide expression profiles, and the intersection of these 500 genes and target genes of the TF.

Additional file 7: Cofactor binding sites adjacent to YY1 and EGR1 sites in the promoters of their targets and non-targets.

Additional file 8: The percentages of positives and negatives whose promoters do not overlap DHSs for the CRISPR-perturbed TFs.

Software availability

Source code implementing the machine learning framework available at: https://bitbucket.org/cytognomix/information-dense-transcription-factor-binding-site-clusters/.

Archived source code at time of publication: https://doi.org/10.5281/zenodo.1892051[48].

Grant information

Natural Sciences and Engineering Research Council of Canada Discovery Grant [RGPIN-2015-06290]; Canada Foundation for Innovation; Canada Research Chairs; Cytognomix Inc. Compute Canada and Shared Hierarchical Academic Research Computing Network (SHARCNET) provided high performance computing and storage facilities. Funding for open access charge: University of Western Ontario and the Natural Sciences and Engineering Research Council.

The funders had no role in study design, data collection and analysis, decision to publish, or preparation of the manuscript.

Acknowledgements

We are grateful to Ben Shirley and Eliseos Mucaki for constructive comments on the paper.

References

1. Hosseinpour B, Bakhtiarizadeh MR, Khosravi P, *et al.*: **Predicting distinct organization of transcription factor binding sites on the promoter regions: a new genome-based approach to expand human embryonic stem cell regulatory network.** *Gene.* 2013; **531**(2): 212–9.
PubMed Abstract | Publisher Full Text
2. Ezer D, Zabet NR, Adryan B: **Homotypic clusters of transcription factor binding sites: A model system for understanding the physical mechanics of gene expression.** *Comput Struct Biotechnol J.* 2014; **10**(17): 63–9.
PubMed Abstract | Publisher Full Text | Free Full Text
3. Lu R, Mucaki EJ, Rogan PK: **Discovery and validation of information theory-based transcription factor and cofactor binding site motifs.** *Nucleic Acids Res.* 2017; **45**(5): e27.
PubMed Abstract | Publisher Full Text | Free Full Text
4. Schneider TD: **Information content of individual genetic sequences.** *J Theor Biol.* 1997; **189**(4): 427–41.
PubMed Abstract | Publisher Full Text
5. Dinakarpandian D, Raheja V, Mehta S, *et al.*: **Tandem machine learning for the identification of genes regulated by transcription factors.** *BMC Bioinformatics.* 2005; **6**: 204.
PubMed Abstract | Publisher Full Text | Free Full Text
6. Ouyang Z, Zhou Q, Wong WH: **ChIP-Seq of transcription factors predicts absolute and differential gene expression in embryonic stem cells.** *Proc Natl Acad Sci U S A.* 2009; **106**(51): 21521–6.
PubMed Abstract | Publisher Full Text | Free Full Text
7. Cheng C, Alexander R, Min R, *et al.*: **Understanding transcriptional regulation by integrative analysis of transcription factor binding data.** *Genome Res.* 2012; **22**(9): 1658–67.
PubMed Abstract | Publisher Full Text | Free Full Text
8. Budden DM, Hurley DG, Cursons J, *et al.*: **Predicting expression: the complementary power of histone modification and transcription factor binding data.** *Epigenetics Chromatin.* 2014; **7**(1): 36.
PubMed Abstract | Publisher Full Text | Free Full Text
9. Smith AD, Sumazin P, Xuan Z, *et al.*: **DNA motifs in human and mouse proximal promoters predict tissue-specific expression.** *Proc Natl Acad Sci U S A.* 2006; **103**(16): 6275–80.
PubMed Abstract | Publisher Full Text | Free Full Text
10. McLeay RC, Lesluyes T, Cuellar Partida G, *et al.*: **Genome-wide *in silico* prediction of gene expression.** *Bioinformatics.* 2012; **28**(21): 2789–96.
PubMed Abstract | Publisher Full Text | Free Full Text
11. Karlić R, Chung HR, Lasserre J, *et al.*: **Histone modification levels are predictive for gene expression.** *Proc Natl Acad Sci U S A.* 2010; **107**(7): 2926–31.
PubMed Abstract | Publisher Full Text | Free Full Text
12. Dong X, Greven MC, Kundaje A, *et al.*: **Modeling gene expression using chromatin features in various cellular contexts.** *Genome Biol.* 2012; **13**(9): R53.
PubMed Abstract | Publisher Full Text | Free Full Text
13. Cusanovich DA, Pavlovic B, Pritchard JK, *et al.*: **The functional consequences of variation in transcription factor binding.** *PLoS Genet.* 2014; **10**(3): e1004226.
PubMed Abstract | Publisher Full Text | Free Full Text
14. Banks CJ, Joshi A, Michoel T: **Functional transcription factor target discovery via compendia of binding and expression profiles.** *Sci Rep.* 2016; **6**: 20649.
PubMed Abstract | Publisher Full Text | Free Full Text
15. Dixit A, Parnas O, Li B, *et al.*: **Perturb-Seq: Dissecting Molecular Circuits with Scalable Single-Cell RNA Profiling of Pooled Genetic Screens.** *Cell.* 2016; **167**(7): 1853–1866.e17.
PubMed Abstract | Publisher Full Text | Free Full Text
16. Cui S, Youn E, Lee J, *et al.*: **An improved systematic approach to predicting transcription factor target genes using support vector machine.** *PLoS One.* 2014; **9**(4): e94519.
PubMed Abstract | Publisher Full Text | Free Full Text
17. Bray JR, Curtis JT: **An Ordination of the Upland Forest Communities of Southern Wisconsin.** *Ecol Monogr.* 1957; **27**(4): 325–349.
Publisher Full Text
18. International Human Genome Sequencing Consortium: **Finishing the euchromatic sequence of the human genome.** *Nature.* 2004; **431**(7011): 931–45.
PubMed Abstract | Publisher Full Text
19. GTEx Consortium: **The Genotype-Tissue Expression (GTEx) project.** *Nat Genet.* 2013; **45**(6): 580–5.
PubMed Abstract | Publisher Full Text | Free Full Text
20. Lu R, Rogan PK: **Information-dense transcription factor binding site clusters identify target genes with similar tissue-wide expression profiles and serve as a buffer against mutations - Source datasets, sample results and compiled software**. 2018.
http://www.doi.org/10.5281/zenodo.1707423
21. Lu R, Rogan PK: **Information-dense transcription factor binding site clusters identify target genes with similar tissue-wide expression profiles and serve as a buffer against mutations - Additional files**. 2018.
http://www.doi.org/10.5281/zenodo.1698281
22. ENCODE Project Consortium: **An integrated encyclopedia of DNA elements in the human genome.** *Nature.* 2012; **489**(7414): 57–74.
PubMed Abstract | Publisher Full Text | Free Full Text
23. Thurman RE, Rynes E, Humbert R, *et al.*: **The accessible chromatin landscape of the human genome.** *Nature.* 2012; **489**(7414): 75–82.
PubMed Abstract | Publisher Full Text | Free Full Text
24. Pearson K: **Note on Regression and Inheritance in the Case of Two Parents.** *Proc R Soc Lond.* 1895; **58**: 240–2.
Publisher Full Text
25. Spearman C: **The Proof and Measurement of Association between Two Things.** *Am J Psychol.* 1904; **15**(1): 72–101.
Publisher Full Text
26. He H, Garcia EA: **Learning from Imbalanced Data.** *IEEE Trans Knowl Data Eng.* 2009; **21**(9): 1263–1284.
Publisher Full Text
27. Kent WJ, Sugnet CW, Furey TS, *et al.*: **The human genome browser at UCSC.** *Genome Res.* 2002; **12**(6): 996–1006.
PubMed Abstract | Publisher Full Text | Free Full Text
28. Sherry ST, Ward MH, Kholodov M, *et al.*: **dbSNP: the NCBI database of genetic variation.** *Nucleic Acids Res.* 2001; **29**(1): 308–11.
PubMed Abstract | Publisher Full Text | Free Full Text
29. Vandevyver S, Dejager L, Libert C: **Comprehensive overview of the structure and regulation of the glucocorticoid receptor.** *Endocr Rev.* 2014; **35**(4): 671–93.
PubMed Abstract | Publisher Full Text
30. Calvo SE, Clauser KR, Mootha VK: **MitoCarta2.0: an updated inventory of mammalian mitochondrial proteins.** *Nucleic Acids Res.* 2016; **44**(D1): D1251–1257.
PubMed Abstract | Publisher Full Text | Free Full Text
31. Cunningham JT, Rodgers JT, Arlow DH, *et al.*: **mTOR controls mitochondrial oxidative function through a YY1-PGC-1alpha transcriptional complex.** *Nature.* 2007; **450**(7170): 736–40.
PubMed Abstract | Publisher Full Text
32. Tallack MR, Perkins AC: **KLF1 directly coordinates almost all aspects of terminal erythroid differentiation.** *IUBMB Life.* 2010; **62**(12): 886–90.
PubMed Abstract | Publisher Full Text
33. Seto E, Lewis B, Shenk T: **Interaction between transcription factors Sp1 and YY1.** *Nature.* 1993; **365**(6445): 462–4.
PubMed Abstract | Publisher Full Text
34. Ferrari-Amorotti G, Mariani SA, Novi C, *et al.*: **The biological effects of C/EBPalpha in K562 cells depend on the potency of the N-terminal regulatory region, not on specificity of the DNA binding domain.** *J Biol Chem.* 2010;

285(40): 30837–50.
PubMed Abstract | Publisher Full Text | Free Full Text

35. Huang RP, Fan Y, Ni Z, *et al.*: **Reciprocal modulation between Sp1 and Egr-1.** *J Cell Biochem.* 1997; **66**(4): 489–99.
PubMed Abstract | Publisher Full Text

36. Bell AC, West AG, Felsenfeld G: **The protein CTCF is required for the enhancer blocking activity of vertebrate insulators.** *Cell.* 1999; **98**(3): 387–96.
PubMed Abstract | Publisher Full Text

37. Hou C, Zhao H, Tanimoto K, *et al.*: **CTCF-dependent enhancer-blocking by alternative chromatin loop formation.** *Proc Natl Acad Sci U S A.* 2008; **105**(51): 20398–403.
PubMed Abstract | Publisher Full Text | Free Full Text

38. Wang LC, Swat W, Fujiwara Y, *et al.*: **The *TEL*/*ETV6* gene is required specifically for hematopoiesis in the bone marrow.** *Genes Dev.* 1998; **12**(15): 2392–402.
PubMed Abstract | Publisher Full Text | Free Full Text

39. Tian L, Liu J, Xia GH, *et al.*: **RNAi-mediated knockdown of MCM7 gene on CML cells and its therapeutic potential for leukemia.** *Med Oncol.* 2017; **34**(2): 21.
PubMed Abstract | Publisher Full Text

40. Maifrede S, Liebermann D, Hoffman B: **Egr-1, a Stress Response Transcription Factor and Myeloid Differentiation Primary Response Gene, Behaves As Tumor Suppressor in CML.** *Blood.* 2014; **124**: 2211.
Reference Source

41. Smith T, Husbands P, Layzell P, *et al.*: **Fitness landscapes and evolvability.** *Evol Comput.* 2002; **10**(1): 1–34.
PubMed Abstract | Publisher Full Text

42. Kimura M: **The neutral theory of molecular evolution.** *Sci Am.* 1979; **241**(5): 98–100, 102, 108 passim.
PubMed Abstract

43. Hural JA, Kwan M, Henkel G, *et al.*: **An intron transcriptional enhancer element regulates IL-4 gene locus accessibility in mast cells.** *J Immunol.* 2000; **165**(6): 3239–49.
PubMed Abstract | Publisher Full Text

44. Vaquerizas JM, Kummerfeld SK, Teichmann SA, *et al.*: **A census of human transcription factors: function, expression and evolution.** *Nat Rev Genet.* 2009; **10**(4): 252–63.
PubMed Abstract | Publisher Full Text

45. Kidder BL, Hu G, Zhao K: **ChIP-Seq: technical considerations for obtaining high-quality data.** *Nat Immunol.* 2011; **12**(10): 918–22.
PubMed Abstract | Publisher Full Text | Free Full Text

46. Shao Y, Chan CY, Maliyekkel A, *et al.*: **Effect of target secondary structure on RNAi efficiency.** *RNA.* 2007; **13**(10): 1631–40.
PubMed Abstract | Publisher Full Text | Free Full Text

47. Lu R, Rogan PK: **Information-dense transcription factor binding site clusters identify target genes with similar tissue-wide expression profiles and serve as a buffer against mutations.** *bioRxiv.* 2018; 283267.
Publisher Full Text

48. Lu R, Rogan PK: **Information dense transcription factor binding site clusters identify target genes with similar tissue-wide expression profiles and buffer against mutations - source code.** *Zenodo.* 2018.
http://www.doi.org/10.5281/zenodo.1892051

Open Peer Review

Current Referee Status: ? ?

Version 1

Referee Report 08 February 2019

https://doi.org/10.5256/f1000research.18988.r42457

? **Nicolae Radu Zabet**
School of Biological Sciences, University of Essex, Colchester, UK

In this manuscript, Ru and Rogan use Bray-Curtis Similarity and several machine-learning algorithms to identify genes that have similar expression patterns. They use transcription factor binding sites within promoter regions and DNA accessibility data to train their models. This is a very important question and the authors propose an interesting mechanistic approach to address it. Nevertheless, there are several limitations that need to be addressed.

Specific comments:

1. While the grammar is at a good level, the way the information is presented makes the text very difficult to read. Some sentences are very long and there are many notations. One suggestion is to move some of the less important parts in the Supplementary Material.
2. On page 3 in the introduction, the authors claim that signal strength of ChIP-seq peaks are not strictly proportional to TF binding strength. This is not always true and we showed in [1] that in fact the number of TF molecules controls the height of the ChIP-seq peak.
3. On page 5, it is not clear why the authors talk of Features 1-3, since it seemed they had 7 features. The way the machine learning information is presented should be improved.
4. The authors test Naïve Bayes, Decision Tree, Random Forest and SVM. I was wondering if they consider also Neural Networks. They don't need to implement that now, but they should at least mention what was behind their selection for the machine-learning algorithms.
5. One of the main findings is that DNA accessibility improves predictions, because it masks potential TF binding sites. This is something that was previously showed in the context of TF binding to the genome by us and other scientists (e.g. References 1,2,3).
6. Figure 4 needs re-plotting (e.g. x axis labels do not fit the figure).
7. In the discussion, none of the statements are referred back to any of the figures in the results section. This makes the reading difficult.
8. The lower performance for YY1 needs to be better explained. The authors claim that this could be explained by lower percentage of negatives in inaccessible promoters. Are there other examples of TFs displaying similar features? What is their performance?
9. One of the main limitations of the manuscript is that the authors use only 82 TFs and claim that there are no iPWM for others. Have they tried to use MotifDB (https://bioconductor.org/packages/release/bioc/html/MotifDb.html), which has approximately 1000 PWMs for human TFs?
10. When talking about the accuracy of the ChIP-seq signal, they could also reference this paper[4].

References
1. Zabet NR, Adryan B: Estimating binding properties of transcription factors from genome-wide binding profiles.*Nucleic Acids Res*. 2015; **43** (1): 84-94 PubMed Abstract | Publisher Full Text
2. Kaplan T, Li XY, Sabo PJ, Thomas S, Stamatoyannopoulos JA, Biggin MD, Eisen MB: Quantitative models of the mechanisms that control genome-wide patterns of transcription factor binding during early Drosophila development.*PLoS Genet*. 2011; **7** (2): e1001290 PubMed Abstract | Publisher Full Text
3. Simicevic J, Schmid AW, Gilardoni PA, Zoller B, Raghav SK, Krier I, Gubelmann C, Lisacek F, Naef F, Moniatte M, Deplancke B: Absolute quantification of transcription factors during cellular differentiation using multiplexed targeted proteomics.*Nat Methods*. 2013; **10** (6): 570-6 PubMed Abstract | Publisher Full Text
4. Teytelman L, Thurtle DM, Rine J, van Oudenaarden A: Highly expressed loci are vulnerable to misleading ChIP localization of multiple unrelated proteins.*Proc Natl Acad Sci U S A*. 2013; **110** (46): 18602-7 PubMed Abstract | Publisher Full Text

Is the work clearly and accurately presented and does it cite the current literature?
Partly

Is the study design appropriate and is the work technically sound?
Yes

Are sufficient details of methods and analysis provided to allow replication by others?
Partly

If applicable, is the statistical analysis and its interpretation appropriate?
Yes

Are all the source data underlying the results available to ensure full reproducibility?
Yes

Are the conclusions drawn adequately supported by the results?
Partly

Competing Interests: No competing interests were disclosed.

Reviewer Expertise: genomics, chromatin biology, transcription regulation, bioinformatics, statistical models,

I have read this submission. I believe that I have an appropriate level of expertise to confirm that it is of an acceptable scientific standard, however I have significant reservations, as outlined above.

Author Response 25 Mar 2019

Peter Rogan, University of Western Ontario, Canada

Comment 1: While the grammar is at a good level, the way the information is presented makes the text very difficult to read. Some sentences are very long and there are many notations. One

suggestion is to move some of the less important parts in the Supplementary Material.
Response: The manuscript has been extensively edited to improve clarity of the presentation. Sentence lengths have been reduced. Duplicate terms and text have been eliminated. All abbreviations have been defined. Two paragraphs have been moved to the Supplementary Methods. The revised manuscript has been shortened by 400 words and approximately 2 pages.

Comment 2: On page 3 in the introduction, the authors claim that signal strength of ChIP-seq peaks are not strictly proportional to TF binding strength. This is not always true and we showed in [1] that in fact the number of TF molecules controls the height of the ChIP-seq peak.
Response: In (1), it was discovered that signal strengths of ChIP-seq peaks are not strictly proportional to strengths (R_i values) of the strongest TFBSs contained in the peaks. The finding in (2) provides a complementary explanation about the determinants of signal strengths of ChIP-seq peaks, which is that 'the number of TF molecules controls the height of the ChIP-seq peak'. Therefore, this sentence is revised to "Because signal strengths of ChIP-seq peaks are not strictly proportional to strengths of the contained strongest TFBSs and are instead controlled by TFBS counts [3, 10], representing…".

Comment 3: On page 5, it is not clear why the authors talk of Features 1-3, since it seemed they had 7 features. The way the machine learning information is presented should be improved.
Response: In this sentence, we would like to make it easier for readers to understand the generation of classifier predictors, by explaining how the seven high-level features were transformed to low-level predictors that were directly input into the classifiers. Therefore, this sentence was revised to "Each of the Features 1-3 was defined in a gene as a vector, whose size equals the number of clusters in the gene promoter; each cluster was mapped to a single value in the vector. In Features 4-7, each cluster itself was mapped to a vector corresponding to binding sites for 82 TFs (Additional file 1)." Also, Section 5 of Additional file 1 gives a specific example about the predictor vector of a gene instance.

Comment 4: The authors test Naïve Bayes, Decision Tree, Random Forest and SVM. I was wondering if they consider also Neural Networks. They don't need to implement that now, but they should at least mention what was behind their selection for the machine-learning algorithms.
Response: We did not select Neural Networks due to two considerations. First, it requires much more data to train than traditional machine learning algorithms, as in at least thousands if not millions of labeled samples (3). In this study the numbers of both positives (i.e. protein-coding genes with similar tissue-wide expression profiles to *NR3C1*) and negatives (i.e. dissimilar genes) are 500, which is insufficient to apply Neural Networks. Second, it is more computationally expensive than traditional algorithms (4).

Comment 5: One of the main findings is that DNA accessibility improves predictions, because it masks potential TF binding sites. This is something that was previously showed in the context of TF binding to the genome by us and other scientists (e.g. References 1,2,3).
Response: Accordingly, in this revision, the last sentence of the second subsection of the Results section was revised to "Consistent with previous findings (2, 5, 6), inclusion of DHS information significantly improved AUC values of the other classifiers with the exception of Naïve Bayes.". And in the second paragraph of the Discussion section, the second sentence was revised to "This intersection eliminated noisy binding sites that are inaccessible to TF proteins in promoters (2, 5, 6),…"

Comment 6: Figure 4 needs re-plotting (e.g. x axis labels do not fit the figure).

Response: In this revision, Figure 4 was replotted to fix this issue.

Comment 7: In the discussion, none of the statements are referred back to any of the figures in the results section. This makes the reading difficult.
Response: In the first paragraph of the Discussion section of this revision, references to the figures in the Results section were added to the following sentences, “In this study, the Bray-Curtis similarity function was initially shown (for the NR3C1 gene) to measure the relatedness of overall expression patterns between genes across a diverse set of tissues (Figure 2). A ML framework distinguished similar from dissimilar genes based on the distribution, strengths and compositions of TFBS clusters in accessible promoters, which can substantially account for the corresponding gene expression patterns (Figures 1 & 3). Using gene expression knockdown data, the combinatorial use of TF binding profiles and chromatin accessibility was also demonstrated to be predictive of TF targets (Figure 4, Tables 2 & 3). A binding site comparison confirmed that coregulatory cofactors can be used to distinguish between functional sites in targets and non-functional ones in non-targets. Furthermore, in silico mutation analyses on binding sites of targets suggested that the existence of both multiple TFBSs in a cluster and multiple information-dense clusters in the same promoter enables both the cluster and the promoter to be resilient to mutations in individual TFBS (Figure 5, Table 5).”

In the third paragraph, references to the figures in the Results section were added to the following sentence, “Mutation analyses revealed that some deleterious TFBS mutations could be compensated for by other information-dense clusters in the same promoter (Figure 5, Table 5)”

Comment 8: The lower performance for YY1 needs to be better explained. The authors claim that this could be explained by lower percentage of negatives in inaccessible promoters. Are there other examples of TFs displaying similar features? What is their performance?
Response: In this sentence, all the seven CRISPR-perturbed TFs were split into two sets; one consisting of only YY1, the other consisting of the remaining six TFs. This sentence was comparing the performances of the Decision Tree classifiers on these two TF sets. Seen from Table 3, the classifier’s performance on YY1 was markedly lower than that on the other six TFs after intersecting promoters with DHS sites, which is due to the fact that YY1 has a smaller percentage of negatives with inaccessible promoters.
To make this clearer, in this revision, this sentence was revised to “Compared to the other six TFs, the poorer performance of the classifier on YY1 (Table 2) is attributable to …”

Comment 9: One of the main limitations of the manuscript is that the authors use only 82 TFs and claim that there are no iPWM for others. Have they tried to use MotifDB (https://bioconductor.org/packages/release/bioc/html/MotifDb.html), which has approximately 1000 PWMs for human TFs?
Response: We selected to use these 94 iPWMs of 82 TFs that were derived from ENCODE ChIP-seq datasets using entropy minimization in (1), since we want to ensure the high quality of the iPWMs used in the analyses.

Compared to the MotifDB PWMs, the reliability and accuracy of these iPWMs were extensively and independently validated using four methods, including detection of experimentally proven binding sites, explanation of effects of characterized SNPs, comparison with previously published motifs and statistical analyses.

These iPWMs were used to scan for 803 experimentally confirmed TFBSs, and there was

complete concordance between these true binding sites and those detected with the iPWMs, both in terms of their locations and relative strengths (1). And these iPWMs were further used to explain the experimentally observed effects of 153 SNPs on binding site strengths, based on the changes in the R_i values. For 130 SNPs (~85.0%), the predictions of the iPWMs and the experimental observations are completely concordant; for 16 SNPs (~10.5%), the predicted and observed experimental findings are concordant, but the extents of these changes differ (e.g. TF binding is predicted to only be weakened, but binding was completely abolished in experiments); for only 7 SNPs (~4.6%), the predicted and observed experimental changes were discordant.

The PWMs in MotifDB are not information theory-based (i.e. not iPWMs). Instead, they are given in the form of count matrices or frequency matrices. The performance of the iPWMs that used in the present study has been shown to outperform other PWM-based approaches for binding site detection and quantification (7).

Comment 10: When talking about the accuracy of the ChIP-seq signal, they could also reference this paper[4].

Response: In this revision, the reference was added to the following sentence in the last paragraph of the Discussion section, “Regarding the CRISPR-generated knockdown data, positives were inferred to be direct targets by intersecting their promoters with corresponding ChIP-seq peaks. This may not be completely accurate, due to the presence of noise peaks that do not contain true TFBSs [3, 50, 51].”

References:

1. Lu,R., Mucaki,E.J. and Rogan,P.K. (2017) Discovery and validation of information theory-based transcription factor and cofactor binding site motifs. *Nucleic Acids Res.*, **45**, e27.
2. Zabet,N.R. and Adryan,B. (2015) Estimating binding properties of transcription factors from genome-wide binding profiles. *Nucleic Acids Res.*, **43**, 84–94.
3. Zhang,Y. and Yang,Q. (2017) A Survey on Multi-Task Learning. *ArXiv170708114 Cs*.
4. Ghodsi,Z., Gu,T. and Garg,S. (2017) SafetyNets: Verifiable execution of deep neural networks on an untrusted cloud. In *Advances in Neural Information Processing Systems*.Vol. 2017-December, pp. 4673–4682.
5. Kaplan,T., Li,X.-Y., Sabo,P.J., Thomas,S., Stamatoyannopoulos,J.A., Biggin,M.D. and Eisen,M.B. (2011) Quantitative models of the mechanisms that control genome-wide patterns of transcription factor binding during early Drosophila development. *PLoS Genet.*, **7**, e1001290.
6. Simicevic,J., Schmid,A.W., Gilardoni,P.A., Zoller,B., Raghav,S.K., Krier,I., Gubelmann,C., Lisacek,F., Naef,F., Moniatte,M., *et al.* (2013) Absolute quantification of transcription factors during cellular differentiation using multiplexed targeted proteomics. *Nat. Methods*, **10**, 570–576.
7. Erill I and O’Neill MC. (2009) A reexamination of information theory-based methods for DNA binding site identification. BMC Bioinformatics, **10**, 57.

Competing Interests: None

Referee Report 09 January 2019

https://doi.org/10.5256/f1000research.18988.r42458

? **Daphne Ezer**
The Alan Turing Institute for Data Science, London, UK

I think that this is an interesting paper that should be published. Often, gene expression patterns are clustered and TF binding sites are used as features to build a classifier for identifying the cluster to which those genes belong or similar schemes such as clustering TFs and gene expression together- see Clements et al[1] and Berman et al[2]. However, a biologist may want to identify what TFs regulate a specific gene of interest. They could then use the 'Bray-Curtis Similarity' index to find a set of genes whose expression pattern is similar to their gene of interest. Then, they can use the pipeline presented here to identify features that are predictive of this kind of gene expression pattern.

They also create a scheme to test how different combinations of features from different experiments influence their predictions.

I think that the text would garner much more interest if it focused more on the research questions that are being addressed. The method details are discussed in depth, but the big picture is hard to find amidst the details.

Main points:

1. One of the main things that bothers me about the Bray-Curtis Similarity metric is that it seems to assume that tissues are independently sampled. However. we see from Fig.1 that there are many brain samples that seem to (at least in the three genes shown) have similar gene expression values. Is there a lot of covariance between gene expression values in pairs of tissues? If so, is there a way to adjust this metric to acknowledge stratification of the tissues. I don't think that the whole paper needs to be re-written with a new metric, but it would be nice if the authors address this directly.
2. Another issue I have is with this metric is that it uses RPKM gene expression values in the Bray-Curtis Similarity metric. Imagine that two genes have extremely high gene expression values in some tissue (like the brain) and low values in another tissue (like the pancreas). However, one of these genes is always expressed at 10 times the level of the other gene. Lets say that a third gene has almost no change of gene expression value across the tissues but has a mean RPKM that is similar to the first gene's mean RPKM. Would the Bray-Curtis SImilarity metric say that gene 1 and 2 are more similar? Or gene 1 and 3? If gene 1 and 3, then this might be resolved by comparing z-scores or otherwise normalising gene expression values across tissues.
3. Every time a machine learning method is named, it should be clear: (1) what are the input features (ii) what are the labels -- i.e. what is being classified (iii) what is the cross-validation or training-testing-validation scheme. Since there are so many machine learning things being done, it is hard sometimes to make sense of what is being done in each specific case.
4. For the method described in (B) in Fig 1: Does it necessarily make sense to compare the 'most similar' to the 'least similar'? Genes that have exactly the opposite gene expression pattern to the one you are interested might be tightly regulated by a different set of TFs. You might be picking up this signal instead of the one you care about! This might be an even bigger issue since you are using raw gene expression values-- genes that are very highly or very lowly expressed in all tissues might always come up in your negative set.

5. Biologists don't just want good classifiers, they want feature selection! Can you show the Gini scores of the features in a supplemental table?

Smaller changes:

1. Is all the code for generating every figure available online? Let's help make research reproducible.
2. If you have 10 values (from cross validation), why don't you show them all in Figure 4 so we can evaluate the spread.
3. "Our *in-silico* mutation analyses revealed that some deleterious TFBS mutations could be compensated for by other information-dense clusters in the same promoter[2]; thus, predicting the effects of mutations in individual binding sites might not be sufficient to interpret downstream effects without considering their context." This is something that me and my collaborators have recently studied[3]. Don't feel pressure to add this citation-- I just thought it would be interesting for you to read! (Also, thanks for discussing IDBC in this paper-- I hadn't heard of it before but it would be relevant to my research.)
4. It would be great if you discussed how Bray-Curtis is used in other fields in the Discussion.
5. Better subsection names in the results section - emphasizing the biological conclusions rather than what was done.

References

1. Clements M, van Someren EP, Knijnenburg TA, Reinders MJ: Integration of known transcription factor binding site information and gene expression data to advance from co-expression to co-regulation. *Genomics Proteomics Bioinformatics*. 2007; **5** (2): 86-101 PubMed Abstract | Publisher Full Text
2. Berman BP, Nibu Y, Pfeiffer BD, Tomancak P, Celniker SE, Levine M, Rubin GM, Eisen MB: Exploiting transcription factor binding site clustering to identify cis-regulatory modules involved in pattern formation in the Drosophila genome.*Proc Natl Acad Sci U S A*. 2002; **99** (2): 757-62 PubMed Abstract | Publisher Full Text
3. Ma X, Ezer D, Adryan B, Stevens T: Canonical and single-cell Hi-C reveal distinct chromatin interaction sub-networks of mammalian transcription factors. *Genome Biology*. 2018; **19** (1). Publisher Full Text

Is the work clearly and accurately presented and does it cite the current literature?
Partly

Is the study design appropriate and is the work technically sound?
Yes

Are sufficient details of methods and analysis provided to allow replication by others?
Yes

If applicable, is the statistical analysis and its interpretation appropriate?
Partly

Are all the source data underlying the results available to ensure full reproducibility?
Yes

Are the conclusions drawn adequately supported by the results?
Partly

Competing Interests: No competing interests were disclosed.

Reviewer Expertise: bioinformatics; transcriptional regulation

I have read this submission. I believe that I have an appropriate level of expertise to confirm that it is of an acceptable scientific standard, however I have significant reservations, as outlined above.

Author Response 25 Mar 2019

Peter Rogan, University of Western Ontario, Canada

Comment 1: One of the main things that bothers me about the Bray-Curtis Similarity metric is that it seems to assume that tissues are independently sampled. However. we see from Fig.1 that there are many brain samples that seem to (at least in the three genes shown) have similar gene expression values. Is there a lot of covariance between gene expression values in pairs of tissues? If so, is there a way to adjust this metric to acknowledge stratification of the tissues. I don't think that the whole paper needs to be re-written with a new metric, but it would be nice if the authors address this directly.
Response: There are 13 brain tissues among all the 53 tissues investigated by GTEx. Admittedly, genes tend to exhibit closer expression values between some of these brain tissues; for example, seen from Figure 2, the *NR3C1* gene has close, low expression values in multiple brain tissues (Amygdala, Anterior cingulate cortex (BA24), Caudate (basal ganglia), etc).

To investigate how much this covariance can influence similarity values between tissue-wide expression profiles of genes computed by the Bray-Curtis function, using the brain tissues as an example, we retained only one brain tissue and removed all other brain tissues at one time, and recomputed the Bray-Curtis similarity values between *NR3C1* and all other protein-coding genes. Thus, there are 13 variant cases due to the presence of 13 brain tissues. Then we compared the resultant set of 500 most similar genes in each variant case to that when all 53 tissues were used (given in Additional file 2).

All of the top 100 most similar genes when using all 53 tissues were among the top 500 genes in every variant case. The top 200 genes when using all 53 tissues differed by 0-3 genes from the top 500 genes in variant cases. The top 500 genes when using all 53 tissues differed by approximately 22% (112-117) from top 500 genes in variant cases. This suggests that the increased number of brain tissues does not significantly influence the results of the Bray-Curtis metric for the most similar genes but does affect results at lower similarity threshold.

Especially, in all 14 cases (i.e. the 13 variant cases and using all 53 tissues), the three most similar genes to *NR3C1* are the same (*SLC25A32*, *TANK*, *CDC27*). Therefore, this covariance between these brain tissues is not a dominant factor in identifying genes with similar tissue-wide expression profiles to a particular gene using the Bray-Curtis Function.

On the other hand, the situation is also present that a gene has closer expression values between two tissues from two different organs, than between two more similar tissues from the same organ. For example, both the Cerebellar Hemisphere (CH) tissue and the Amygdala tissue are from the brain; the Visceral Adipose (VA) tissue and the Adrenal Gland (AG) tissue are not. Seen from Figure 2, for the *NR3C1* gene's expression, there is a larger difference between CH and Amygdala. Instead, CH is closer to VA, whereas Amygdala is closer to AG.

Despite well established developmental lineages for these tissues, we prefer not to make

assumptions regarding the covariance in expression values between similar tissues from the same organ. The null hypothesis should not discriminate between tissues or weight them differently, without explicit prior information about tissue-specific expression, which is what we are trying to measure. For this reason, when computing similarity values between tissue-wide expression profiles of genes using the Bray-Curtis Function or other metrics, it may be more appropriate to assign the same weight to every tissue and treat every tissue equally.

Comment 2: Another issue I have is with this metric is that it uses RPKM gene expression values in the Bray-Curtis Similarity metric. Imagine that two genes have extremely high gene expression values in some tissue (like the brain) and low values in another tissue (like the pancreas). However, one of these genes is always expressed at 10 times the level of the other gene. Lets say that a third gene has almost no change of gene expression value across the tissues but has a mean RPKM that is similar to the first gene's mean RPKM. Would the Bray-Curtis SImilarity metric say that gene 1 and 2 are more similar? Or gene 1 and 3? If gene 1 and 3, then this might be resolved by comparing z-scores or otherwise normalising gene expression values across tissues.

Response:
Gene 1 and 3 will be more similar according to Bray-Curtis Similarity. The inference is as follows:
Assume that there are two tissues t_1 and t_2. The expression values of Gene 1 in the two tissues are [a, b] (b>>a>0), the expression values of Gene 2 are [10a, 10b], and the expression values of Gene 3 are [(a+b)/2, (a+b)/2].
Then the Bray-Curtis similarity value between Gene 1 and Gene 2 is:
$sim_{BC}\ (G1,G2) = 2/11$.
The Bray-Curtis similarity value between Gene 1 and Gene 3 is:
$sim_{BC}\ (G1,G3) = (3a+b)/(2a+2b)$.
Thus, $sim_{BC}\ (G1,G3) > sim_{BC}\ (G1,G2)$.

However, this is not unreasonable. In other words, this is not a problem, thus it does not need to be resolved. There is no ground-truth relationship between $sim_{BC}\ (G1,G2)$ and $sim_{BC}\ (G1,G3)$. The reason is described below.

When measuring the similarity between two vectors, there are two factors to be considered: 1. the sizes of the vectors (i.e. the distance between the two vectors), 2. the directions of the vectors (i.e. the angle between the two vectors). In this context of measuring similarity between tissue-wide expression values of genes (each gene is mapped to a vector), both factors matter.

It is stated in the Methods section that Bray-Curtis Similarity satisfies three desirable properties. In fact, Property 2 (achieving the maximal similarity value 1 if and only if two vectors are identical) ensures Factor 1 to be considered, and Property 3 (larger values having a larger impact on the resultant similarity value) ensures Factor 2 to be considered.

Thus, Table 1 shows that Bray-Curtis Similarity is more appropriate than the other five metrics, which is exactly due to the fact it takes both factors into account. In contrast, Euclidean Similarity does not take vectors' directions into account; Cosine Similarity, Pearson Correlation and Spearman Correlation do not take the sizes of the vectors into account.

Thus, to be able to infer a ground-truth similarity relationship, on both Factor 1 and Factor 2 the intuitive comparison results must be concordant. In Example 1 (see Additional File 1), the angle between Gene *A* and Gene *C* is identical to that between Gene *B* and Gene *C*, and the distance

between *A* and *C* is larger than that between *B* and *C*; thus, *sim (A,C) < sim (B,C)*. Similarly, the distance between *A* and *D* is identical to that between *E* and *F*, and the angle between *A* and *D* is larger than that between *E* and *F*; thus, *sim(A,D) < sim(E,F)*.

But in this case, the distance between Gene 1 and Gene 2, i.e. 9*sqrt($a^2 + b^2$), is larger than that between Gene 1 and Gene 3, i.e. (*b*-*a*)/sqrt(2), but the angle between Gene 1 and Gene 2 (i.e. 0) is smaller than that between Gene 1 and Gene 3 (>0). Thus, a ground-truth similarity relationship is unable to be inferred.
Thus, the result given by Bray-Curtis Similarity, i.e.sim_{BC} *(G1,G3)* > sim_{BC} *(G1,G2),* is not unreasonable.

Comment 3: Every time a machine learning method is named, it should be clear: (1) what are the input features (ii) what are the labels -- i.e. what is being classified (iii) what is the cross-validation or training-testing-validation scheme. Since there are so many machine learning things being done, it is hard sometimes to make sense of what is being done in each specific case.

Response: In the module to predict genes with similar tissue-wide expression profiles to a particular gene, to make these points clearer, the following changes were made:

(i) Using the red color Figure 1A shows that seven features were derived from TFBS clusters. In addition, in the legend of Figure 1A, the following sentence was added “The seven ML features derived from TFBS clusters were described in the Methods section.” The second paragraph of the second subsection of the Methods section details the seven features; its first sentence was revised to “The seven information density-related ML features derived from each TFBS cluster included …”

(ii) The first sentence of the ‘Prediction of genes with similar tissue-wide expression profiles” subsection of the Methods section was revised’ to ‘The framework for predicting whether the tissue-wide expression profile of a gene resembles a particular gene is indicated in Figure 1A, B.”, so that it is clear that the two labels are ‘similar to the particular gene’ and ‘dissimilar to the particular gene’. In addition, Figure 1B also indicates that 500 most similar genes and 500 most dissimilar genes were selected as positives and negatives.

(iii) The last step (‘Performance evaluation’) of Figure 1A was revised to ‘Performance evaluation (ROC curve/10-fold cross validation)’; the red color indicates that ROC curves were used to validate the classifiers in this module. In addition, the last sentence of the legend of Figure 1A was revised to “The performance of ML classifiers was evaluated with ROC curves and 10-fold cross validation”.

The last sentence of the second subsection of the Methods section was revised to “This allowed all genes to be used as training data for ML classifiers. Default parameter values for these classifiers were used to generate ROC curves in MATLAB”, and also the first sentence of the corresponding second subsection of the Results section was revised to “Several ML classifiers (Naïve Bayes, Decision Tree (DT), Random Forest and Support Vector Machines (SVM) with four different kernels) were evaluated to determine how well TFBS-related features could predict genes with tissue-wide expression profiles similar to NR3C1. Their performance were compared using ROC curves…”. Thus, it is now clear that ROC curves were used to validate the classifiers and all instances were used as training data (i.e. there were no test sets).

In the module to predict TF target genes, to make these points clearer, the following changes were

made:

(i) Using the blue color Figure 1A shows that six features were derived from TFBS clusters. Also, the penultimate sentence of the last paragraph of the “Using gene expression in the CRISPR-based perturbations” subsection of the Methods section states “Six features (Features 1-5 and 7) were derived from each homotypic cluster (i.e. Feature 6 became identical to Feature 3, because only binding sites from a single TF were used) (Figure 1A).”. Combining with the detailed descriptions about what the features are in the second paragraph of the previous subsection, it is clear that these six features (Features 1-5 and 7) were used.

(ii) The last sentence of the first paragraph of the ‘Using gene expression in the CRISPR-based perturbations” subsection of the Methods section was revised to “We defined a positive TF target gene in a cell line as:…” And the sentence in the fifth paragraph was revised to “If the coefficients of all guide RNAs of the TF for a gene are zero, the gene was defined as a negative (i.e. a non-target gene).” Thus it is clear that the two labels are “TF target genes” and “non-target genes”. Combining with the last sentence of the first paragraph of the Methods section, ‘Since protein-coding (PC) sequences represent the most widely studied and best understood component of the human genome [19], positives and negatives for deriving machine learning classifiers for predicting DE direct TF target genes that encode proteins (TF targets, below) were obtained from CRISPR- and siRNA-generated knockdown data’, it is clear that the ‘target genes’ here stands for ‘PC, direct, DE target genes’.

(iii) As stated above, the last step (‘Performance evaluation’) of Figure 1A was revised to ‘Performance evaluation (ROC curve/10-fold cross validation)’; the blue color indicates that 10- fold cross validations were used to validate the classifiers in this module. In addition, the last sentence of the legend of Figure 1A was revised to “The performance of ML classifiers was evaluated with ROC curves and 10-fold cross validation”. The last sentence of the last paragraph of the “Using gene expression in the CRISPR-based perturbations” subsection of the Methods section was revised to “The results of 10 rounds of 10-fold cross validation were averaged to evaluate the accuracy of the classifier.” Thus it is clear that the validation scheme is 10-fold cross validation.

Comment 4: For the method described in (B) in Fig 1: Does it necessarily make sense to compare the 'most similar' to the 'least similar'? Genes that have exactly the opposite gene expression pattern to the one you are interested might be tightly regulated by a different set of TFs. You might be picking up this signal instead of the one you care about! This might be an even bigger issue since you are using raw gene expression values-- genes that are very highly or very lowly expressed in all tissues might always come up in your negative set.:

Response: Yes, it makes sense. As stated in the above response to Comment 3, in this module to predict genes with similar tissue-wide expression profiles to a particular gene, the two labels are ‘similar to the given gene’ and ‘dissimilar to the given gene’. Therefore, it makes the most sense that the most similar genes were selected as positives and the most dissimilar genes were selected as negatives.

The first sentence of the last paragraph of the Background section, “…the distribution and composition of *cis*-regulatory modules in promoters substantially determines gene expression profiles…, is exactly the underlying rationale why this machine learning framework is able to distinguish between “similar genes” and “dissimilar genes”. In other words, “similar genes” and “dissimilar genes” have different expression patterns, presumably because they have different

organizations and compositions (i.e. different TF sets) of TFBSs in their promoters. Therefore, the potential fact that “similar genes” and “dissimilar genes” are regulated by different TF sets was exactly what we expected to see and validate.

Comment 5: Biologists don't just want good classifiers, they want feature selection! Can you show the Gini scores of the features in a supplemental table?:

Response: In the module to predict TF target genes based on CRISPR- and siRNA-generated knockdown data, to assess the relative importance of the six features to the Decision Tree classifiers, we computed their Gini importance values, which are added to Additional file 5.

For the seven CRISPR-perturbed TFs in the K562 cell line, the cluster-level Features 1-3, especially Feature 3 capturing the information density of TFBS clusters, have the largest contribution to the classifiers’ predictive power. By contrast, for the 11 siRNA-perturbed TFs in the GM19238 cell line, the binding site-level Feature 5 capturing the spatial distribution of strong TFBSs has the largest contribution.

Accordingly, in this revision, this observation is described in the second and third sentences of the first paragraph of the third subsection of the Results section.

Comment 6: Is all the code for generating every figure available online? Let's help make research reproducible.

Response: As stated in the Software availability section, the code that implemented this machine learning framework and produced all the results has been deposited at https://bitbucket.org/cytognomix/information-dense-transcription-factor-binding-site-clusters/src and https://doi.org/10.5281/zenodo.1892051. The input of the code to derive the figures is directly taken from the output of the ML framework code. There are no intermediate steps or variable required to generate the figures in MATLAB.

The code for generating the figures is used to visualize the results. in this revision, we also deposited the MATLAB code for generating all the figures at https://bitbucket.org/cytognomix/information-dense-transcription-factor-binding-site-clusters/src

Comment 7: If you have 10 values (from cross validation), why don't you show them all in Figure 4 so we can evaluate the spread.

Response: To avoid making Figure 4 too complicated, in this revision, the accuracy values of all individual rounds of 10-fold cross validations in prediction of TF target genes were added to Additional file 5. Accordingly, the legends of Table 2, Figure 4 and Table 3 were revised to indicate this.

Comment 8: "Our in-silico mutation analyses revealed that some deleterious TFBS mutations could be compensated for by other information-dense clusters in the same promoter(2); thus, predicting the effects of mutations in individual binding sites might not be sufficient to interpret downstream effects without considering their context." This is something that me and my collaborators have recently studied3. Don't feel pressure to add this citation-- I just thought it would be interesting for you to read! (Also, thanks for discussing IDBC in this paper-- I hadn't heard of it before but it would be relevant to my research.)

Response: In this revision, this publication has now been referenced (number 47) in the manuscript.

Comment 9: It would be great if you discussed how Bray-Curtis is used in other fields in the Discussion.

Response:The following sentences were added to the penultimate paragraph, “Previous applications of this index include: a) measurement of the ecological transfer of species abundance from dense to sparse plots [48] and comparative difference analyses of species quantities between reference and algorithm-derived metagenomic sample mixtures (https://precision.fda.gov/challenges/3/view/results). b) improvement of friend recommendation in geosocial networks by using it to compare users’ movement history [49, 50] ..”

Comment 10: Better subsection names in the results section - emphasizing the biological conclusions rather than what was done.
Response: In the Results section of this revision, the title of each subsection was revised as follows, now summarizing the primary conclusion from this subsection.

The title of the first subsection was revised from ‘Similarity between GTEx tissue-wide expression profiles of genes’ to ‘The Bray-Curtis Function can accurately quantify the similarity between tissue-wide gene expression profiles’.

The title of the second subsection was revised from ‘Prediction of genes with similar GTEx tissue-wide expression profiles’ to ‘The Decision Tree classifier performed best in prediction of genes with similar tissue-wide expression profiles’.

The title of the third subsection was revised from ‘Prediction of TF targets” to ‘The Decision Tree classifier was predictive of TF target genes’.

The title of the fourth subsection was revised from ‘Intersection of genes with similar tissue-wide expression profiles and TF targets’ to ‘Some TF target genes also display similar tissue-wide expression profiles to the TFs, themselves.

The title of the fourth subsection was revised from ‘Mutation analyses on promoters of direct targets’ to ‘Transcription factor binding site clusters buffer against expression changes from mutations in single sites’.

Competing Interests: none